



*Ετήσια Επιστημονική
Συνεδρία της ΕΓΕ*



*Σπόγγοι και μητρικά πετρώματα υγρών και
αερίων υδρογονανθράκων*

Δρ. Μανούσογλου Εμμανουήλ

Γεωλόγος

Καθηγητής

Τμήματος Μηχανικών Ορυκτών Πόρων

Πολυτεχνείου Κρήτης

- “About 70% of the total world petroleum resources are concentrated in the Tethyan realm, the Mesozoic deposits being the most prolific source rocks of these oil and gas reserves. To understand the depositional controls of these organic-rich facies at the scale of the Tethys is a challenging problem.”

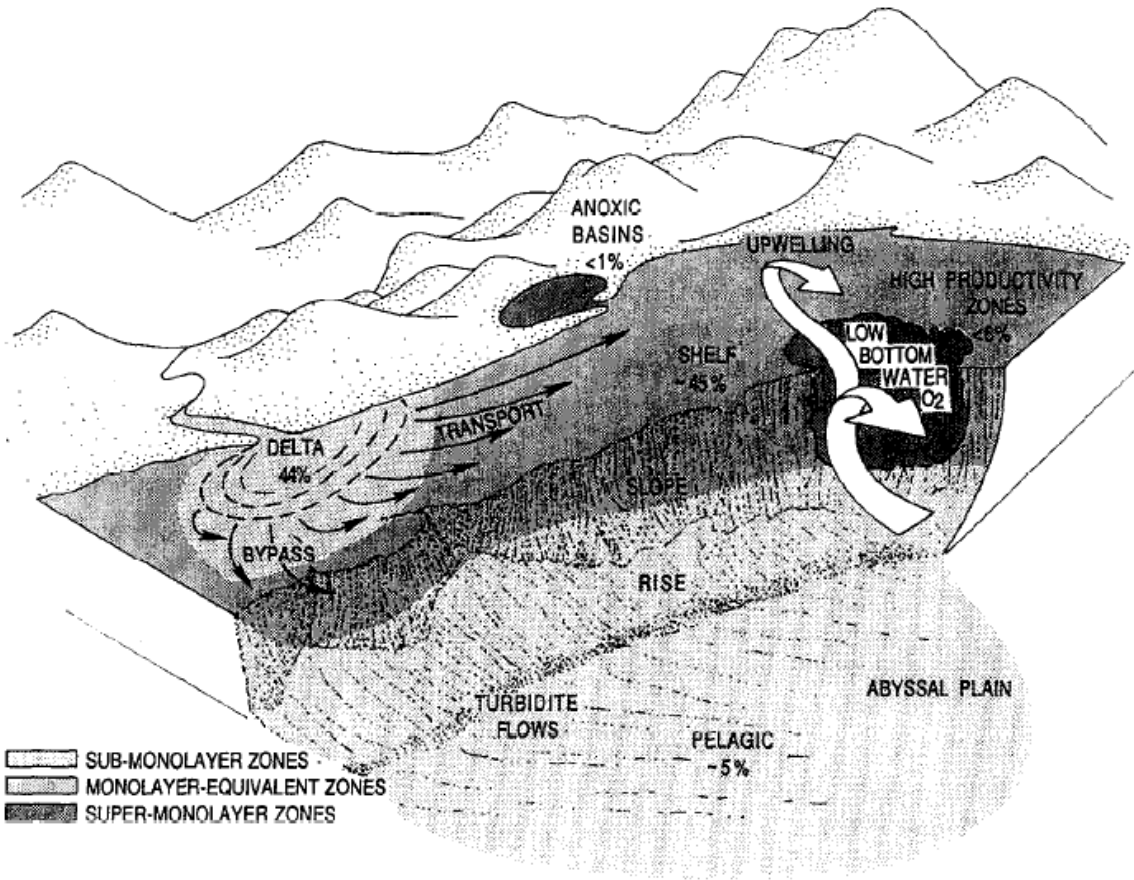
François Baudin (1995): Depositional Controls on Mesozoic Source Rocks in the Tethys. – In: Paleogeography, Paleoclimate, and Source Rocks [Edit. A-Y. Huc], AAPG Studies in Geology, No. 40, 191-212.

Major reservoirs of inorganic and organic carbon

Reservoir type	Amount ^a	Reference
Sedimentary rocks		
<i>Inorganic</i>		
Carbonates	60,000	Berner (1989)
<i>Organic</i>		
Kerogen, coal, etc.	15,000	Berner (1989)
Active (surficial) pools		
<i>Inorganic</i>		
Marine DIC	38	Olson et al. (1985)
Soil carbonate	1.1	Olson et al. (1985)
Atmospheric CO ₂	0.66	Olson et al. (1985)
<i>Organic</i>		
Soil humus ^b	1.6	Olson et al. (1985)
Land plant tissue ^b	0.95	Olson et al. (1985)
Seawater DOC	0.60	Williams and Druffel (1987)
Surface marine sediments	0.15	Emerson and Hedges (1988)

^a Unit = 10¹⁸ g C

^b Values corrected to levels before anthropogenic effects.



Idealized diagram depicting current estimates of the percentage of total organic matter burial occurring within various marine sediment types, *J.I. Hedges, R.G. Keil/Marine Chemistry 49 (1995) 81-115*

Oceanic productivity	50 X 10¹⁵ grC yr⁻¹
sediment burial rates	0.16 X 10¹⁵ grC yr⁻¹
Organic preservation in the marine environment	<0.5%
Shelf	~45%
Delta	44%
High productivity zones	<6%
Pelagic	~5%
Anoxic Basins	1%

J.I. Hedges, R.G. Keil/Marine Chemistry 49 (1995) 81-115

- Most marine primary productivity occurs in the open ocean, by rapidly growing phytoplankton....
- ..are continuously grazed by protozoans and zooplankton
- 20% of net primary production falls as particles
- 10% of surficial productivity remaining at depths of several hundred meters
- only 1% passing to an average ocean depth of 4000 m
- Rivers provide the major conduit towards the preservation of OC in marine sediment
- Carbon-rich deposits tend to be the focal point of the debate between proponents of anoxia- vs. productivity-induced preservation of organic matter

J.I. Hedges, R.G. Keil/Marine Chemistry 49 (1995) 81-115

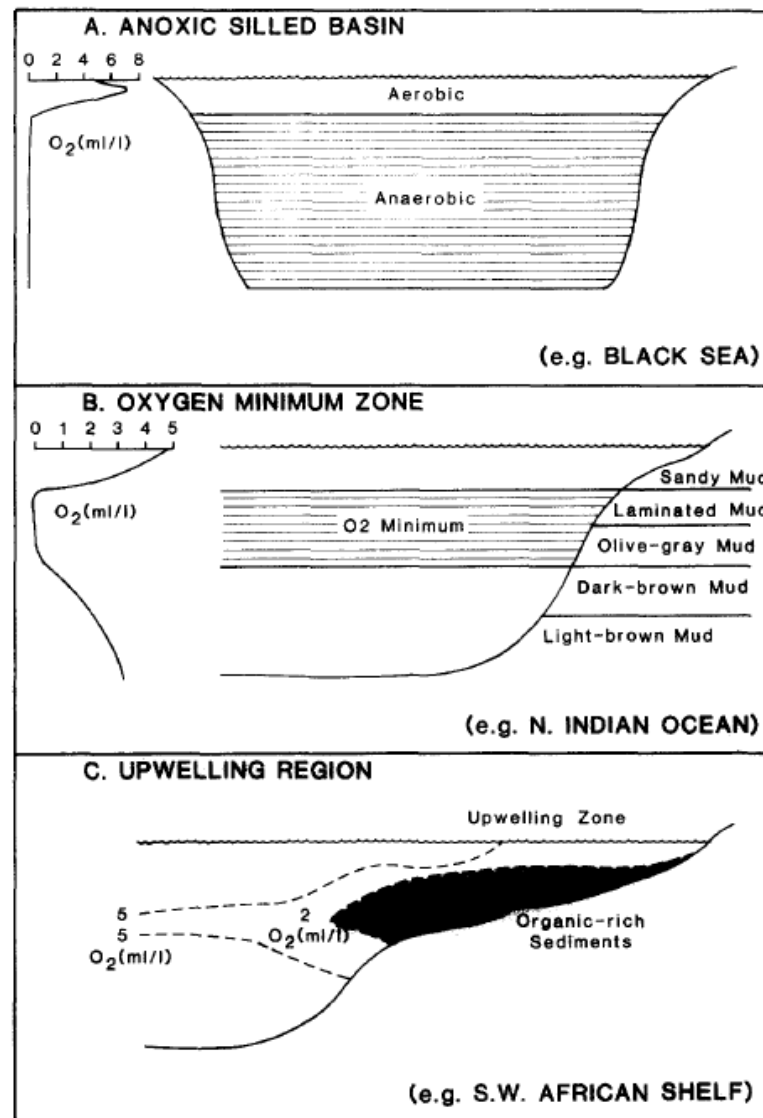
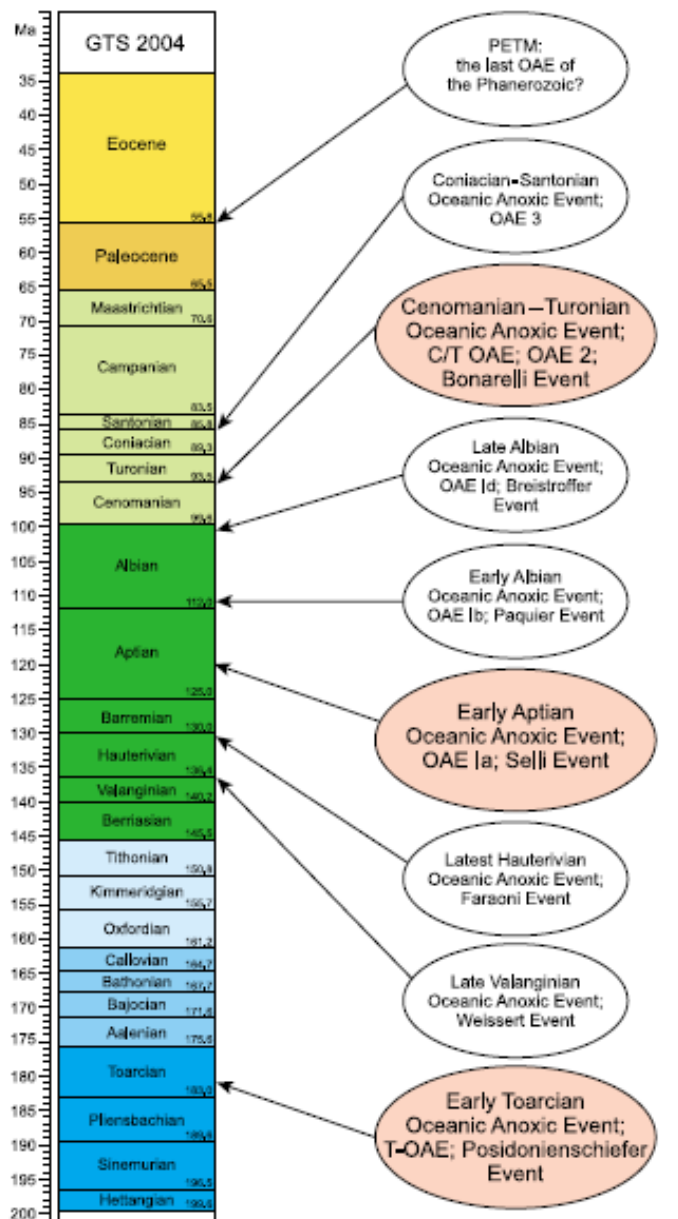


Fig.1. General models for the deposition of organic-rich sediments. A. Anoxic silled basin of the Black Sea type (after Thiede and Van Anel, 1977). B. Oxygen-minimum zone impinging on the continental margin (after Von Stackelberg, 1972; and Thiede and Van Anel, 1977). C. Upwelling regions such as that found on the African shelf off of Namibia (after Demaison and Moore, 1980).

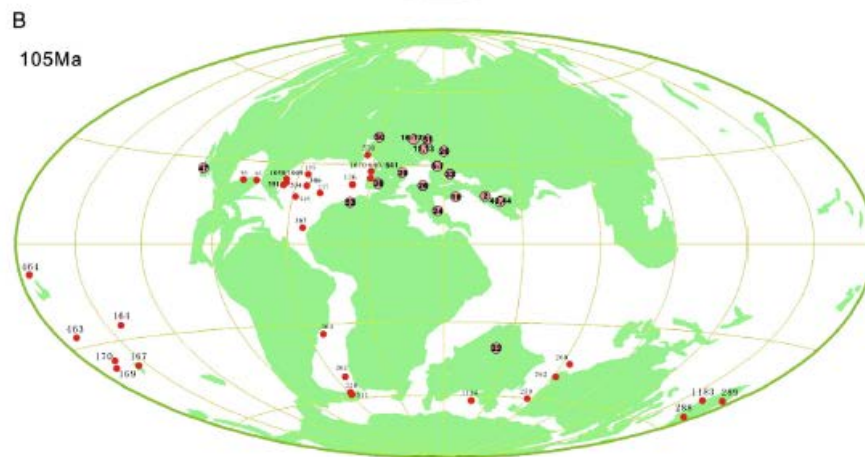
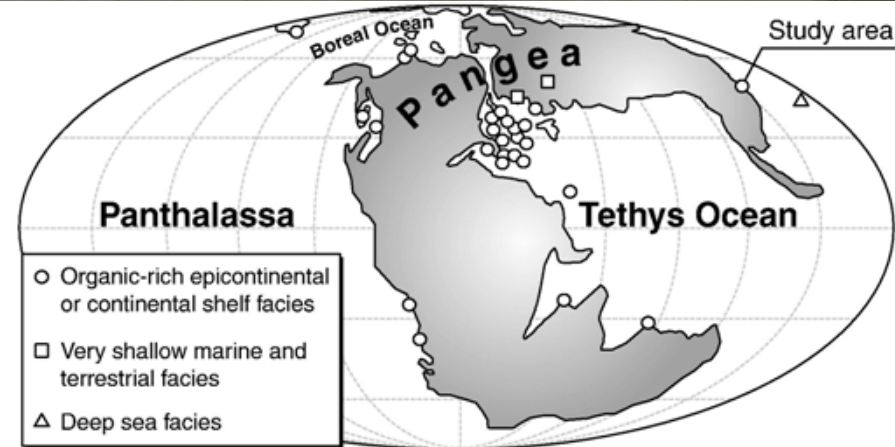
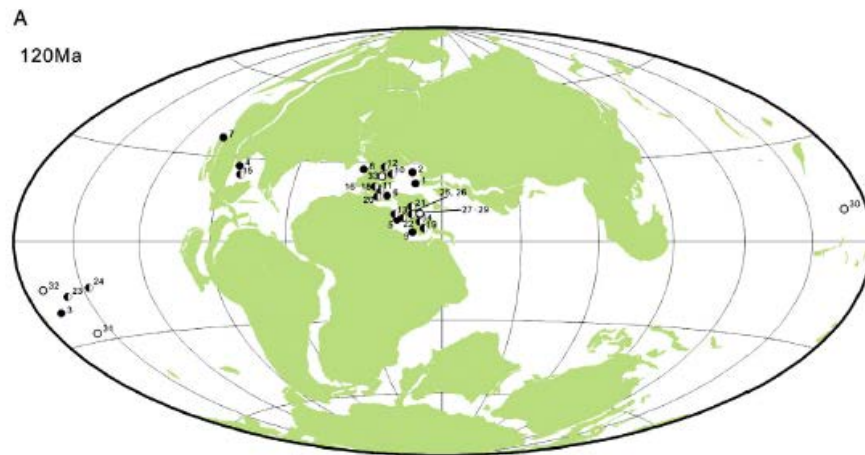


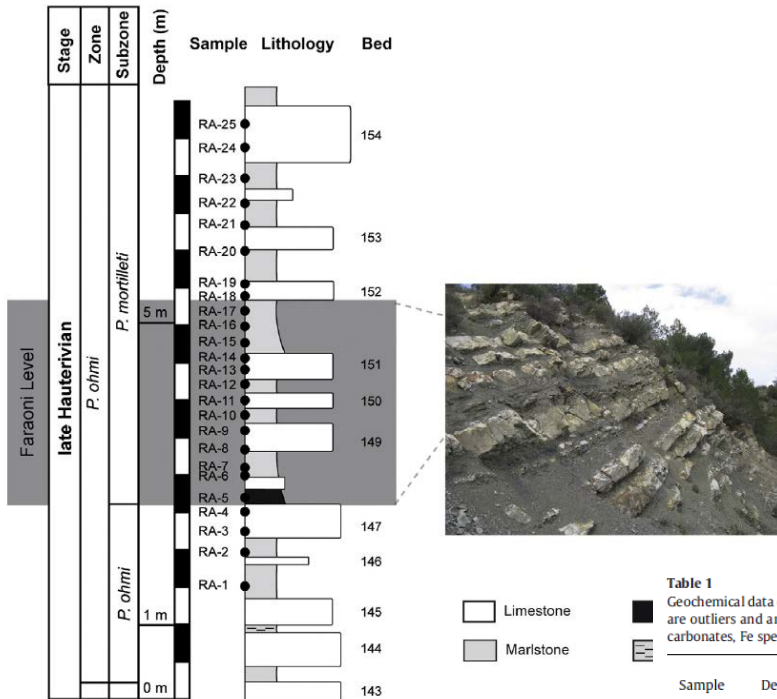
Fig. 1. Paleogeographic map showing the occurrence of OAE1a and CORBs at 120 Ma and 105 Ma. A) Distribution of OAE1a, early Aptian (120 Ma) data from published literature (Appendix 1), keys for the symbols: ● – all three characteristics features of black shales, a high content of OM and excursions of $\delta^{13}C$; ◐ – two of the three characteristics features; ○ – one of the three characteristics features; B) Distribution of CORBs at 105 Ma cited from Wang et al. (2009). The paleogeographic base map was downloaded from the website www.odm.de.

The global distribution of lower Toarcian bituminous black shales

Izumi et al. / *Palaeogeography, Palaeoclimatology, Palaeoecology* 315-316 (2012) 100–108

Wang et al. / *Sedimentary Geology* 235 (2011) 27–37

The late Hauterivian Faraoni “Oceanic Anoxic Event” at Río Argos (southern Spain): An assessment on the level of oxygen depletion, Sauvage et al. / Chemical Geology 340 (2013) 77–90



□ Limestone
■ Marlstone

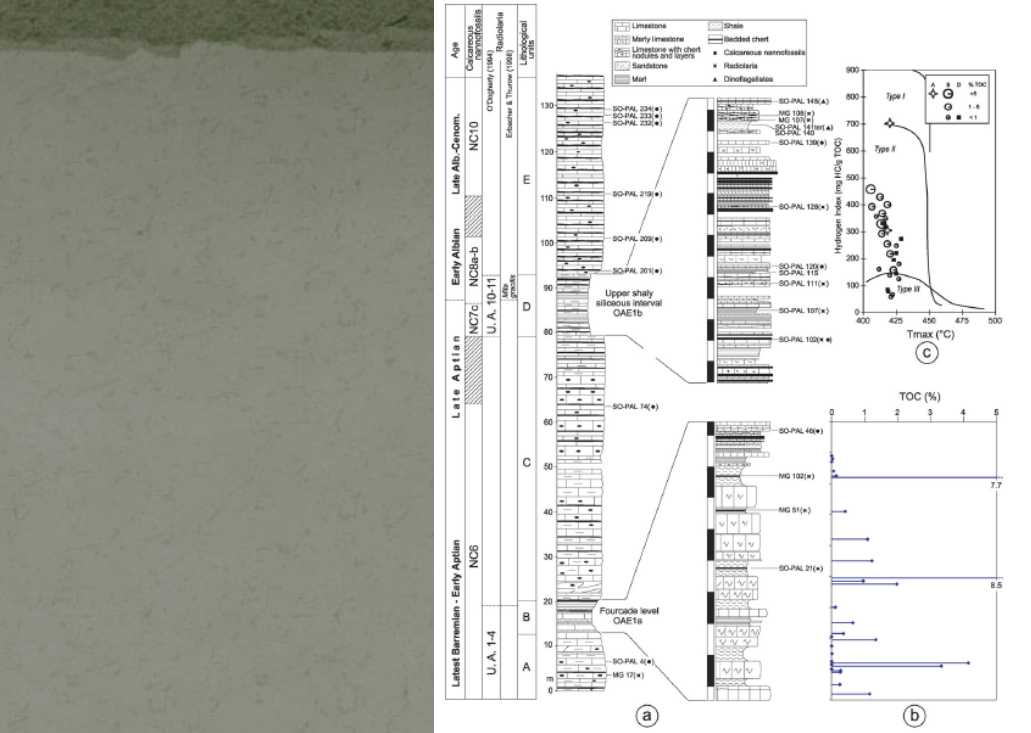
Table 1

Geochemical data of the Río Argos X.Ag1 study section. The gray band indicates the Faraoni Level. Missing values are measurements below the detection limit. Values in parentheses are outliers and are not considered in the discussion section. The mean value and the Standard Deviation (SD, 1σ) of different proxies (CaCO_3 , Rock-Eval values, $\delta^{13}\text{C}$ and $\delta^{18}\text{O}$ of carbonates, Fe speciation values, Al) and element/Al are indicated in *italics*.

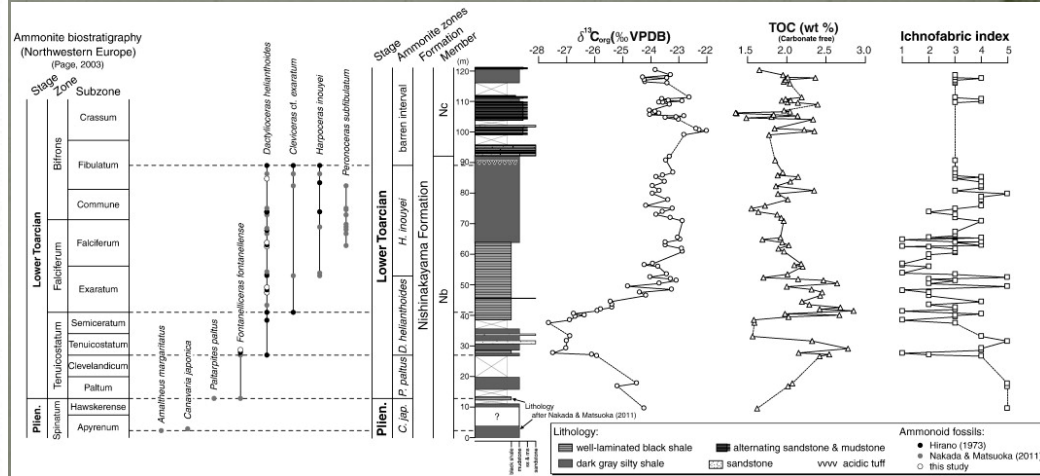
Sample	Depth (m)	Lithology	CaCO_3 (%)	TOC (wt.%)	HI (mg HC / g TOC)	OI (mg CO_2 / g TOC)	Tmax ($^\circ\text{C}$)	$\delta^{13}\text{C}$ (‰ to V-PDB)	$\delta^{18}\text{O}$ (‰ to V-PDB)	6N HCl: Fe_T (ppm)	ICP-MS: Fe_T (ppm)	Δ (%) ^a	[Fe_{carb}] (ppm)	[Fe_{org}] (ppm)
RA-1	1.58	Marlstone	52.5	0.09	106	167	421	1.23	-2.36	17,038	17,766	4.1	1466	1663
RA-2	1.98	Marlstone	59.0	0.48	136	75	428	1.39	-2.58	15,703	16,926	7.2	1221	2214
RA-3	2.38	Limestone	92.5	(0.04)	(275)	(713)	(429)	1.61	-1.86	6882	7834	12.1	1776	56
RA-4	2.58	Limestone	93.0	0.05	(67)	(150)	(418)	1.60	-2.19		9792		2222	504
RA-5	2.78	Marlstone	67.0	1.53	234	115	429	1.31	-2.86	19,496	19,514	0.1	1323	8789
RA-6	2.98	Marlstone	73.5	0.10	80	40	428	1.21	-2.70		12,730		1578	2454
RA-7	3.18	Marlstone	65.0	0.09	(44)	(533)	(430)	1.32	-2.57	12,205	13,429	9.1	1343	2343
RA-8	3.35	Limestone	81.5	(0.03)	(100)	(367)	(425)	1.42	-2.40	9055	9932	8.8	1198	1290
RA-9	3.58	Limestone	95.5	0.05	(70)	(910)	(328)	1.68	-1.98	8742	7344	-19.0	1762	386
RA-10	3.78	Marlstone	55.5	0.08	75	12	421	1.33	-2.67	17,234	18,325	6.0	779	2403
RA-11	3.98	Limestone	84.5	(0.04)	(75)	(275)	(434)	1.72	-2.27	11,801	13,009	9.3	1559	1735
RA-12	4.18	Marlstone	59.0	0.17	76	65	423	1.47	-2.95	14,975	16,996	11.9	1583	1239
RA-13	4.43	Limestone	93.5	(0.03)	(142)	(1200)	(402)	1.65	-2.44	7029	8953	21.5	1929	1364
RA-14	4.63	Limestone	90.5	0.05	(80)	(540)	(432)	1.73	-2.78	8590	9023	4.8	2085	530
RA-15	4.83	Marlstone	69.5	0.13	62	208	427	1.54	-2.81	12,566	13,569	7.4	1765	830
RA-16	5.03	Marlstone	79.5	0.08	(59)	(2172)	(412)	1.70	-2.71	11,384	12,380	8.0	2191	677
RA-17	5.23	Marlstone	72.5	0.09	122	189	426	1.58	-2.64	13,396	13,989	4.2	1578	1570
RA-18	5.33	Limestone	91.5	(0.03)	(100)	(750)	(449)	1.72	-2.44	9134	9372	2.5	2003	1589
RA-19	5.53	Limestone	89.0	(0.04)	(75)	(525)	(430)	1.71	-2.63	8853	9163	3.4	2207	748
RA-20	5.93	Marlstone	53.5	0.09	44	222	429	1.12	-2.98	14,647	20,144	27.3	1212	2251
RA-21	6.33	Marlstone	66.5	0.13	92	(0)	423	1.36	-2.92	14,350	14,758	2.8	1666	1162
RA-22	6.63	Marlstone	51.0	0.12	50	50	422	0.96	-2.93	18,130	20,773	12.7	1128	1809
RA-23	6.93	Marlstone	60.0	0.08	(50)	(288)	(423)	1.20	-2.81	20,350	20,563	1.0	974	6904
RA-24	7.33	Limestone	89.0	(0.02)	(17)	(1000)	(522)	1.06	-2.82	8500	8883	4.3	1577	1825
RA-25	7.73	Limestone	93.5	(0.02)	(25)	(1675)	469	0.51	-3.14		8113		1389	2169
Mean value of X/Al			75.11	0.15	98	114	428	1.41	-2.62	12,730	0.50		1581	1940
SD (1σ)			15.45	0.30	53	77	3	0.29	0.32	4109	0.10		390	1925



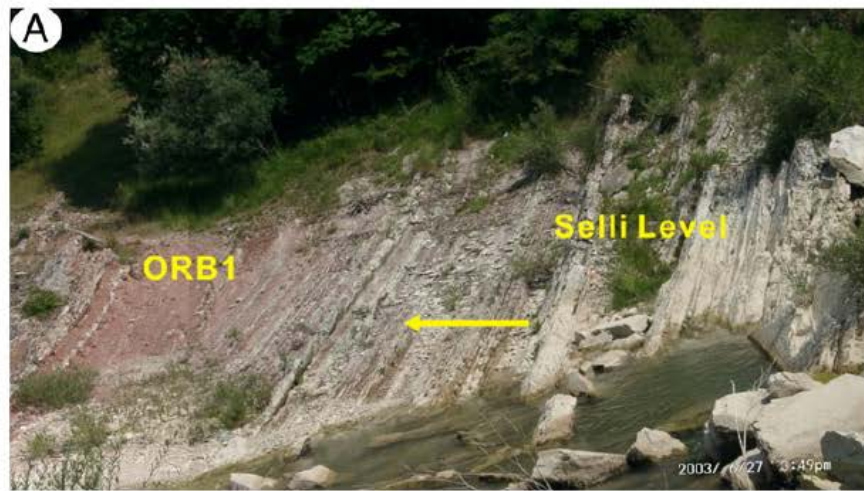
Cretaceous Research, 28, (2007) 597-612



Revue de Micropaleontologie 50 (2007) 225–237



Izumi et al. / Palaeogeography, Palaeoclimatology, Palaeoecology 315-316 (2012) 100–108



Wang et al. / Sedimentary Geology 235 (2011) 27–37

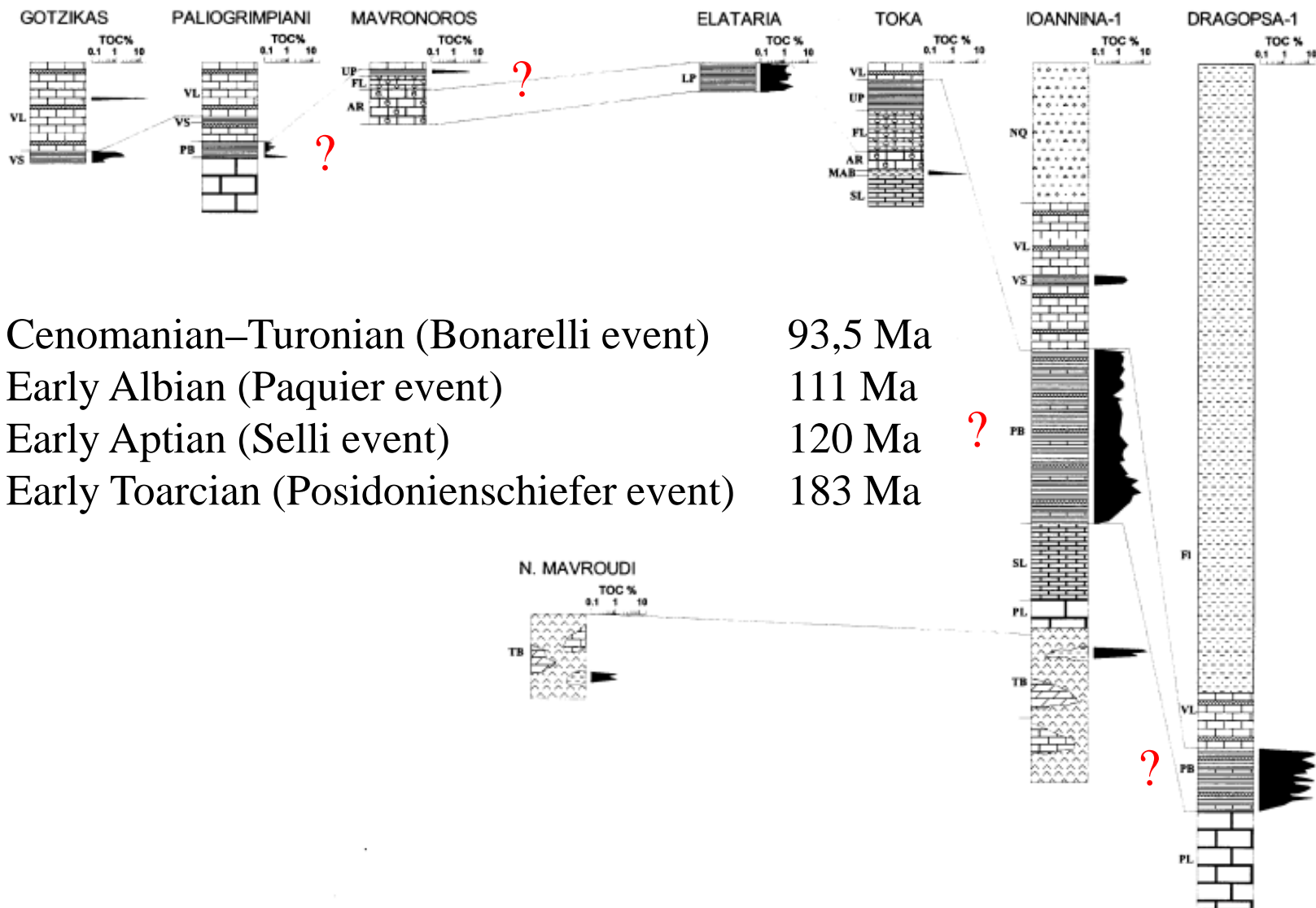
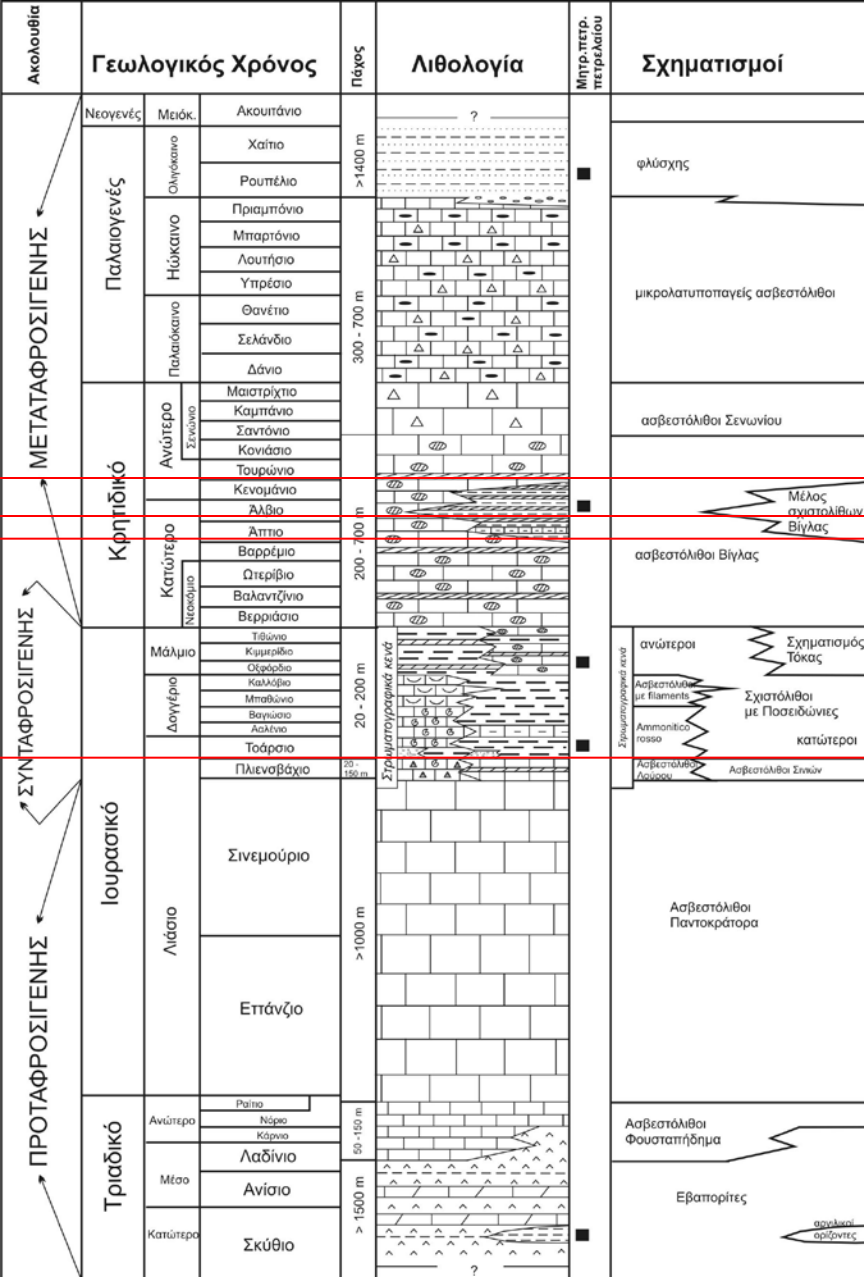
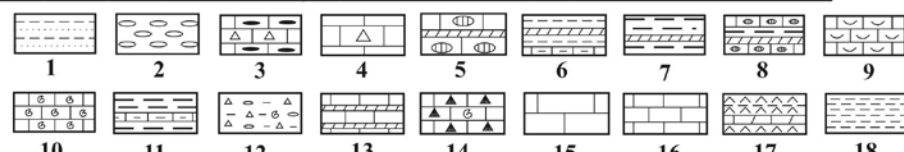


Fig. 3. Selected lithological sections and wells and vertical distribution of organic matter in the Ionian Zone, Epirus (location of the sections and wells in Fig. 1): NQ, quaternary and Neogene; FL, Flysch; VL, Vigla Limestones; VS, Vigla Shales; UP, Upper Posidonia Beds; FL, Limestones with filaments; LP, Lower Posidonia Beds; AR, Ammonitico Rosso; MAB, Marls at the base of AR; PB, undifferentiated Posidonia Beds; SL, Sinia's Limestones; PL, Pantolcrator Limestones; TB, Triassic breccias.



	Ασβεστόλιθοι Βίγλας	Ασβεστόλιθοι Ανώτ. Σενωνίου			Ασβεστόλιθοι Παλαιοκ.- Ηώκαιου
		Συνολικά	Φάση II	Φάση III	
Περιοχή 1	1,1	1,1	0,9	1,3	1,7
Περιοχή 2	1,7	1,5	1,2	1,3	1,3
Περιοχή 3	1,2	1,4	0,7	2,4	0,9
Περιοχή 4	1,0	1,6	0,9	1,9	1,0
Περιοχή 5	1,1	0,8	0,8	1,2	0,7
Περιοχή 6	1,2	0,9	1,3	0,9	0,6
Μέσος όρος	1,2	1,2	1,0	1,5	1,0

Μέσος όρος πορώδους (%) ανά σχηματισμό στην περιοχή της Ηπείρου, από Μπακόπουλο 2006, Δ.Δ. ΕΚΠΑ

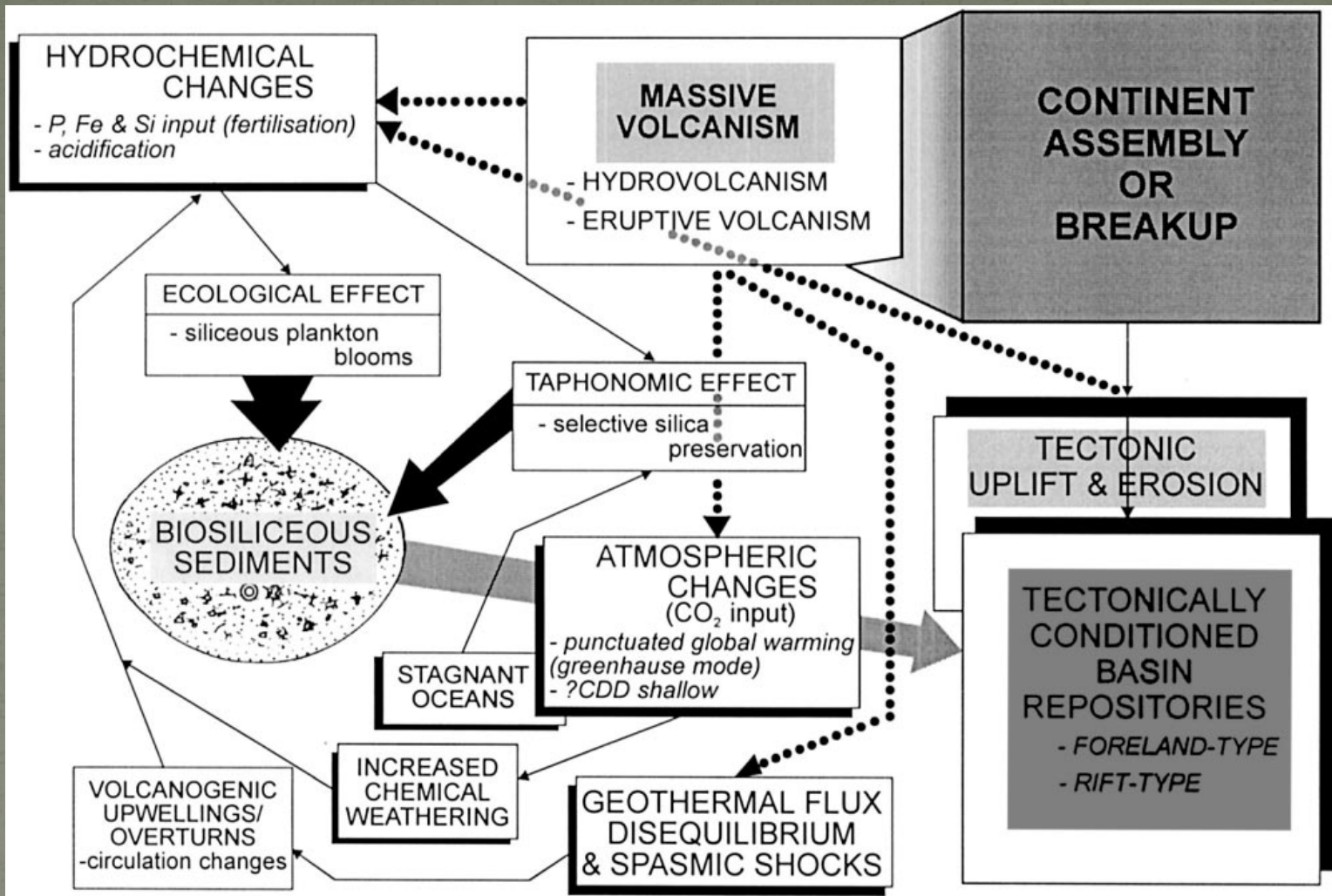


← Από Karakitsios & Rigakis 2007, JPG, 30, 197-218

Στον χώρο των Εξωτερικών Ελληνίδων εμφανίζεται από το Μέσο Τριαδικό αλλά κυρίως μετά το Ιουρασικό, μια συζυγία πετρωμάτων πυριτικής σύστασης στις Ζώνες Πίνδου, Ιόνιος, Παξών καθώς και στα μεταμορφωμένα πετρώματα των Πλακωδών Ασβεστολίθων (Πελοπόννησος, Κρήτη, Κάσος, Κάρπαθος, Ρόδος).

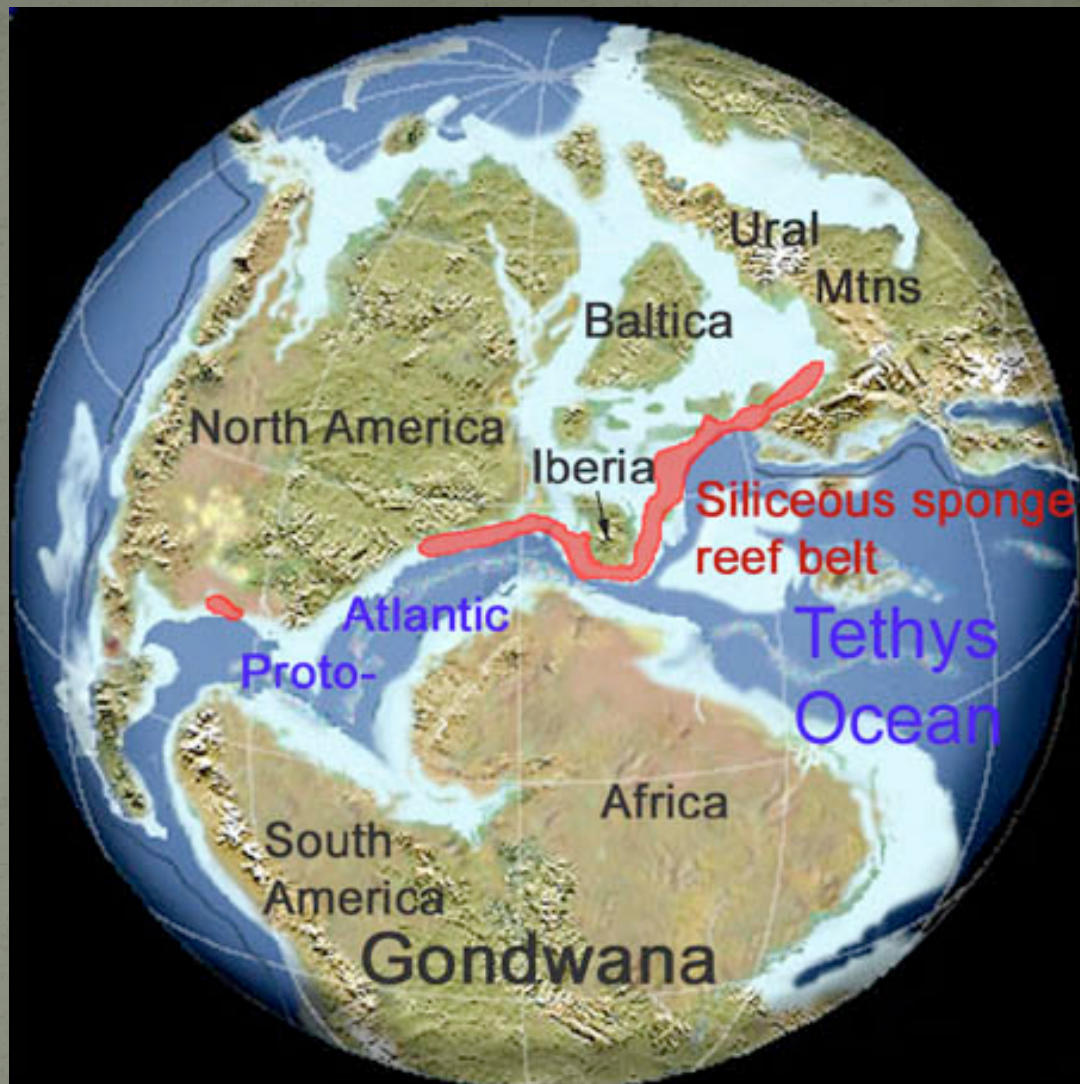
Ορισμοί - Ερμηνείες

- Πυριτόλιθοι - κερατόλιθοι
Ανόργανης (διαγενετικής) προέλευσης
ή
- “Ραδιολαρίτες”

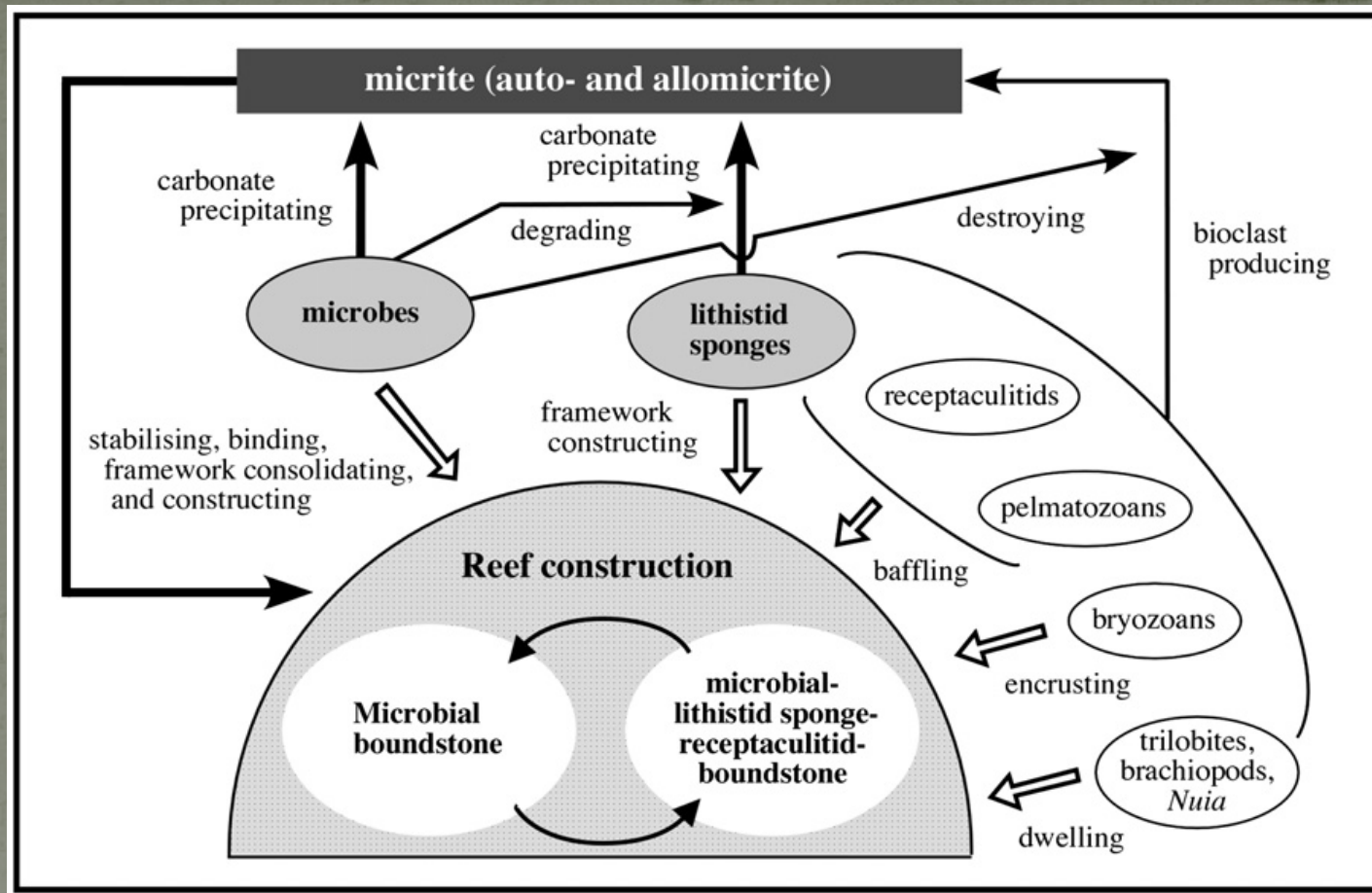


Flow chart for the model of massive volcanism and tectonics as a main control of biosiliceous sedimentation

Ύφαλοι πυριτιοσπόγγων έχουν εμφανιστεί διαδοχικά στην εξελικτική πορεία του πλανήτη. Στο Ανώτερο όμως Ιουρασικό σχημάτισαν μια υφαλογόνο αλυσίδα που επεκτάθηκε πάνω από 7.000 χιλ. Ο σημερινός ύφαλος που υπάρχει (Great Barrier Reef) στην Αυστραλία είναι σχετικά μικρός σε σχέση με αυτόν του Ανωτέρου Ιουρασικού. Το σύστημα αυτό των υφάλων αποτέλεσε την μεγαλύτερη βιοτική δομή που δημιουργήθηκε ποτέ πάνω στην Γη.



Paleogeographic situation during Late Jurassic.
(Map used and modified after Blakey 2002)

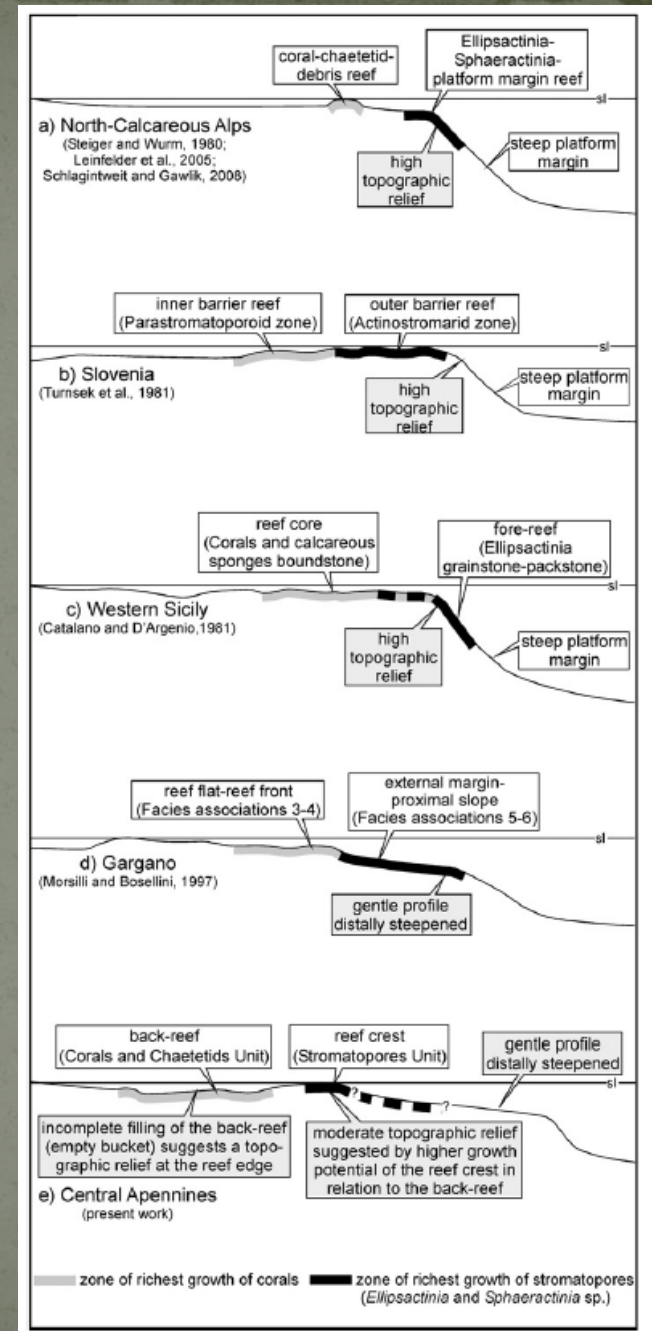


Schematic model showing those elements that combined to construct the Lower Ordovician reefs, made up of microbial boundstones and microbial-lithistid sponge-receptaculitid boundstones. Micrites are a significant component of the reefs and are produced variously by microbes as well as skeletal organisms (lithistid sponges in particular).

“The Late Jurassic records is one of the largest reefal expansions of the Phanerozoic, with a greater diffusion and differentiation in the Tethys realm”

Comparison of main morphological features and distribution of main biota along the depositional profiles of available examples from Intra-Tethys reef types

..zonation model for Upper Jurassic Intra-Tethys reef complexes, Rusciadelli et al. / *Sedimentary Geology* 233 (2011) 69–87



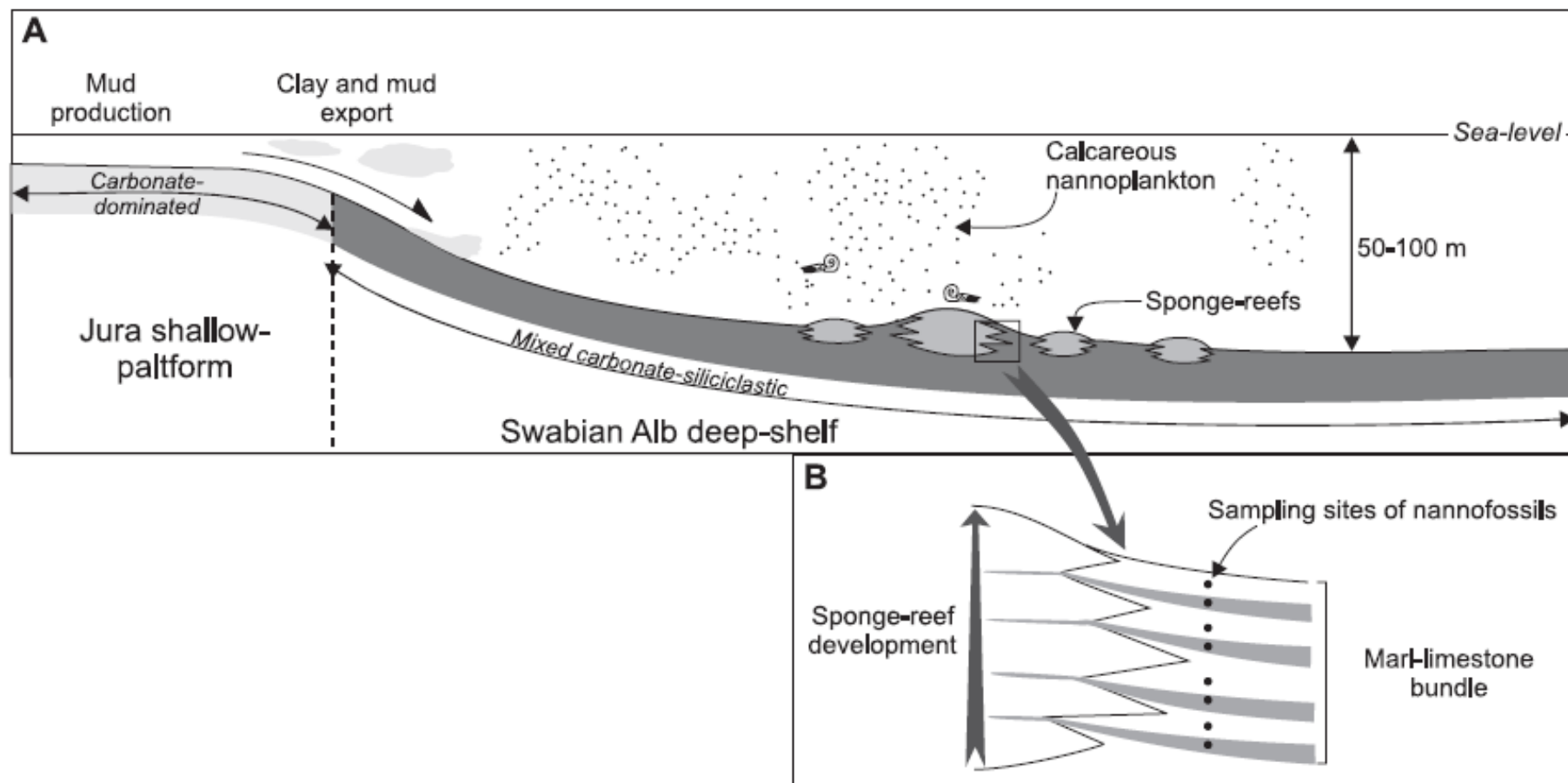


Fig. 4. (A) Schematic reconstruction of the Swabian deep-shelf setting during the Oxfordian. This deep-shelf environment is characterised by an abundant sponge-microbialite-reef development. The mixed carbonate-siliciclastic deposits characteristic of Upper Oxfordian deep-shelf settings record both calcareous nannoplankton accumulations and the export of carbonate mud from the adjacent, shallow, carbonate-dominated Jura platform (Pittet and Mattioli, 2002). (B) Sketch showing the close relationships between the successive reef-growth phases and the lateral marl-limestone bundles that record a variable amount of calcareous nannofossils. Laterally to the sponge-microbialite reef, each limestone bed and marly level were sampled for calcareous nannofossil analysis.

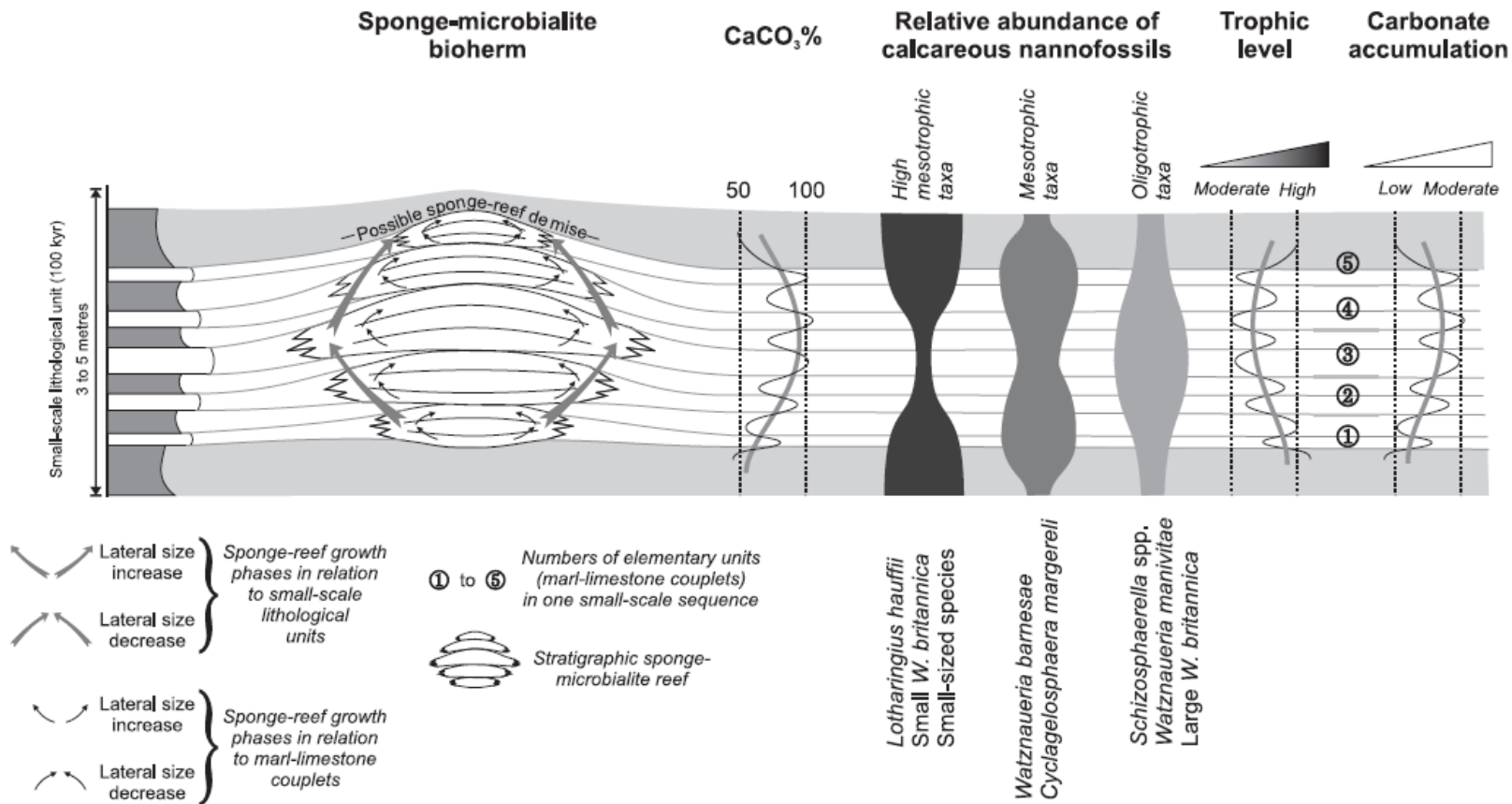
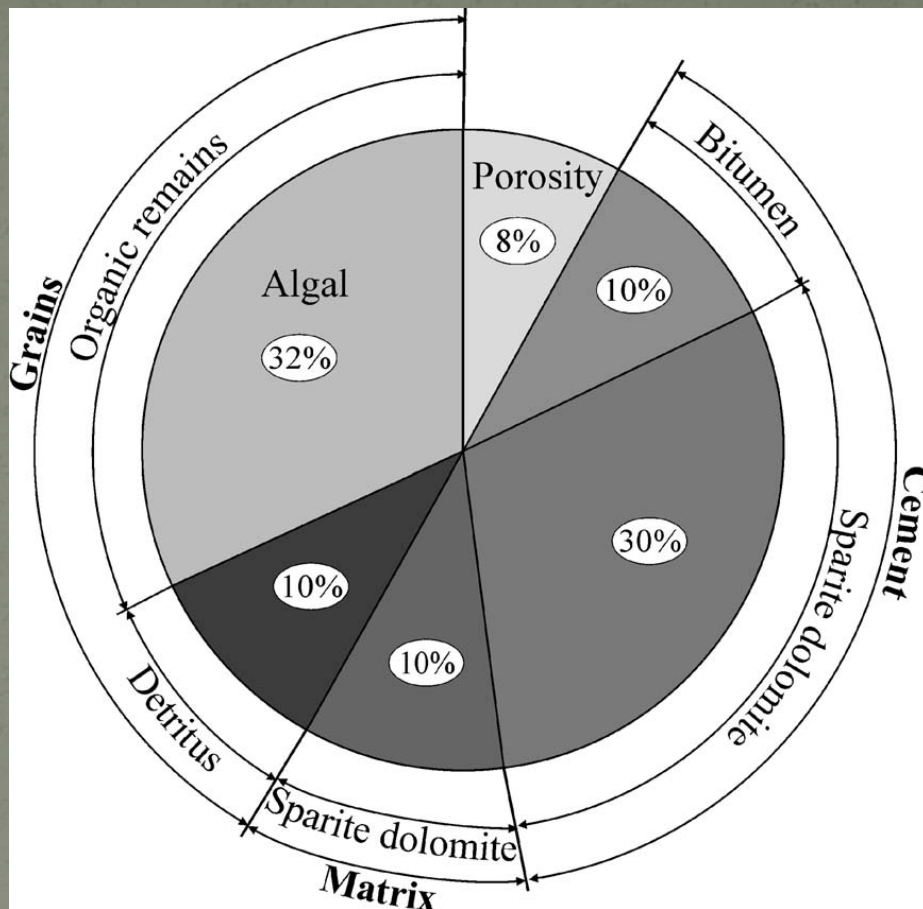


Fig. 14. Model for the development of individual sponge build-ups in marl-dominated deposits driven by trophic level and carbonate accumulation in the Swabian deep-shelf.

- “The sediment within the sponge bioherms is characterized by a high levels of organic carbon. The large amount of organic carbon (**more than 3 weight percent**) found in the reef sediments is similar to that found at modern deltas on the west coast of Canada (Bornhold, 1978). Reducing conditions, which are usually observed in the recovered cores and grab samples in the shallow subsurface in reef sediments, are probably explained by this high organic carbon content. These dys- or anoxic conditions are responsible for the paucity and low diversity of endobenthic organisms” (Recent Hexactinellid Sponge Reefs on the Continental Shelf of British Columbia, Canada, <http://www.porifera.org/a/cif1.htm>)

The link between black cherts and high biological activity is nearly systematic from the Precambrian to the Recent (van Kranendonk, 2001)

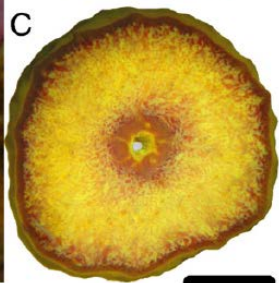
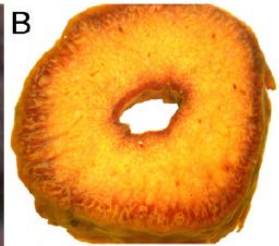


Organogenic build-up

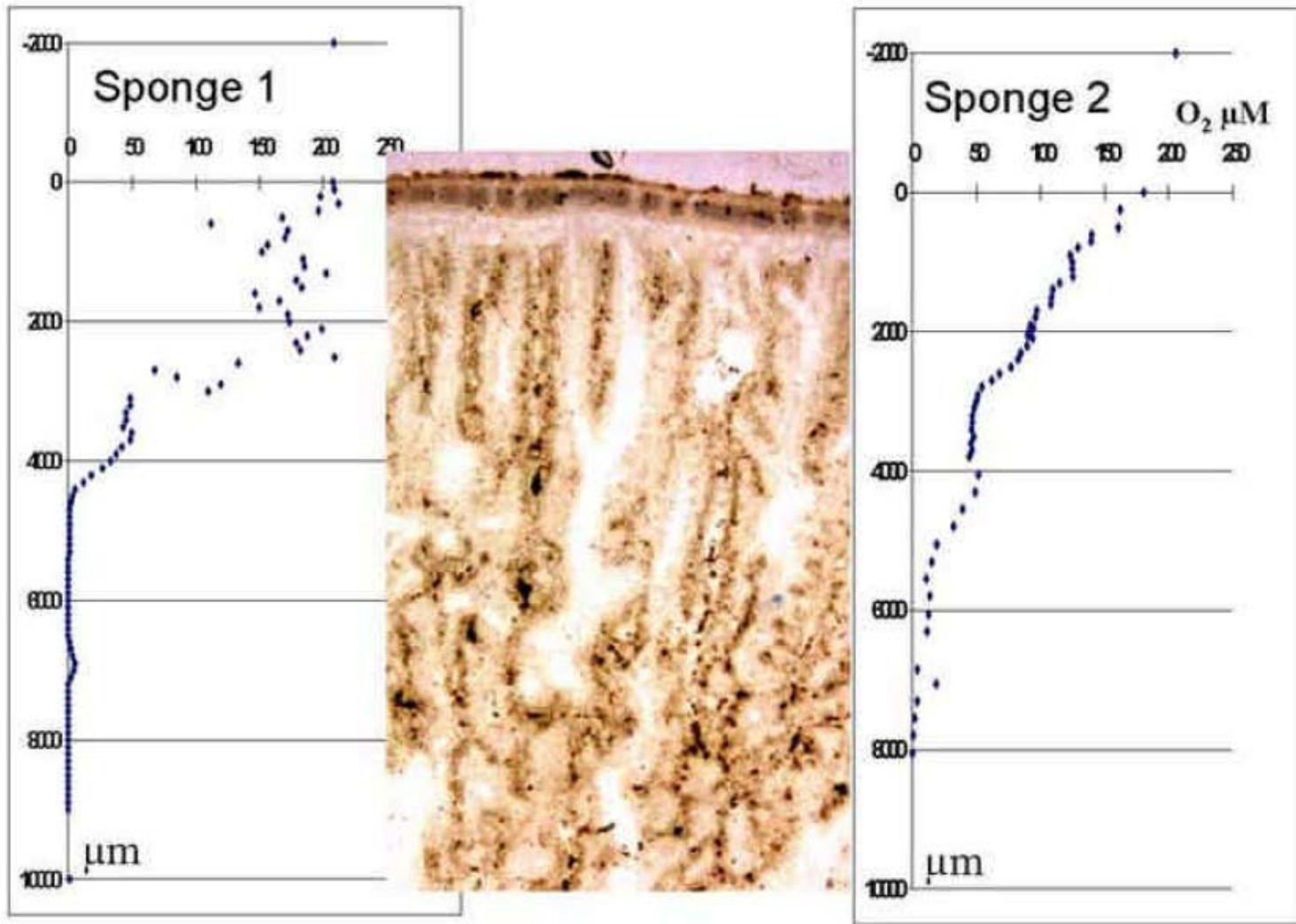
(Organic remain: algae, stromatoporoids, crinoids, gastropods, protozoans)

A lithofacies model for the Upper Devonian Pamyatno-Sasovskoye **reef (oilfield)** (Volgagraskoe Povolzhye, Russia)

S.V. Deliya, N.V. Danshina / Palaeoworld 19 (2010) 278–283

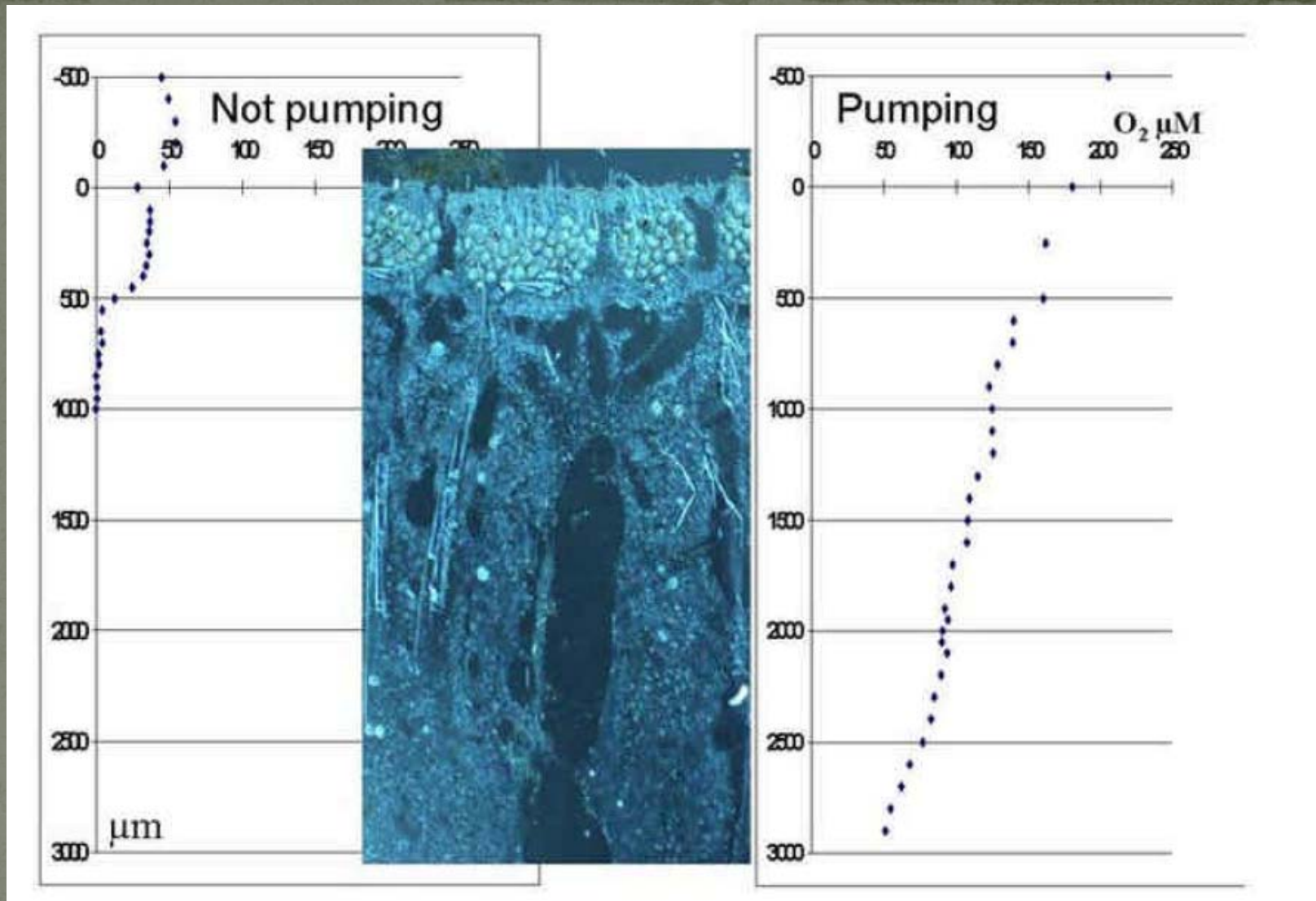


Journal of Experimental Marine Biology and Ecology,
369 (2009) 65–71



Oxygen profiles 1 cm into the tissue of two pumping *G. barretti* related to a microscopical sponge section of the same scale.

Microbial sulfate reduction in the tissue of the cold-water sponge Geodia barretti (Tetractinellida, Demospongiae), Hoffmann F., *Dissertation*, Göttingen, 2003

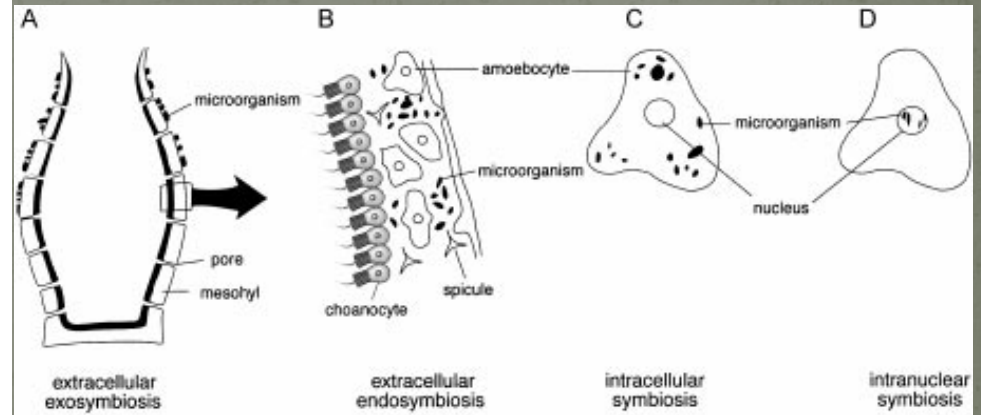


Oxygen profiles 3 mm into the tissue of sponge 2, related to a microscopical sponge section of the same scale.

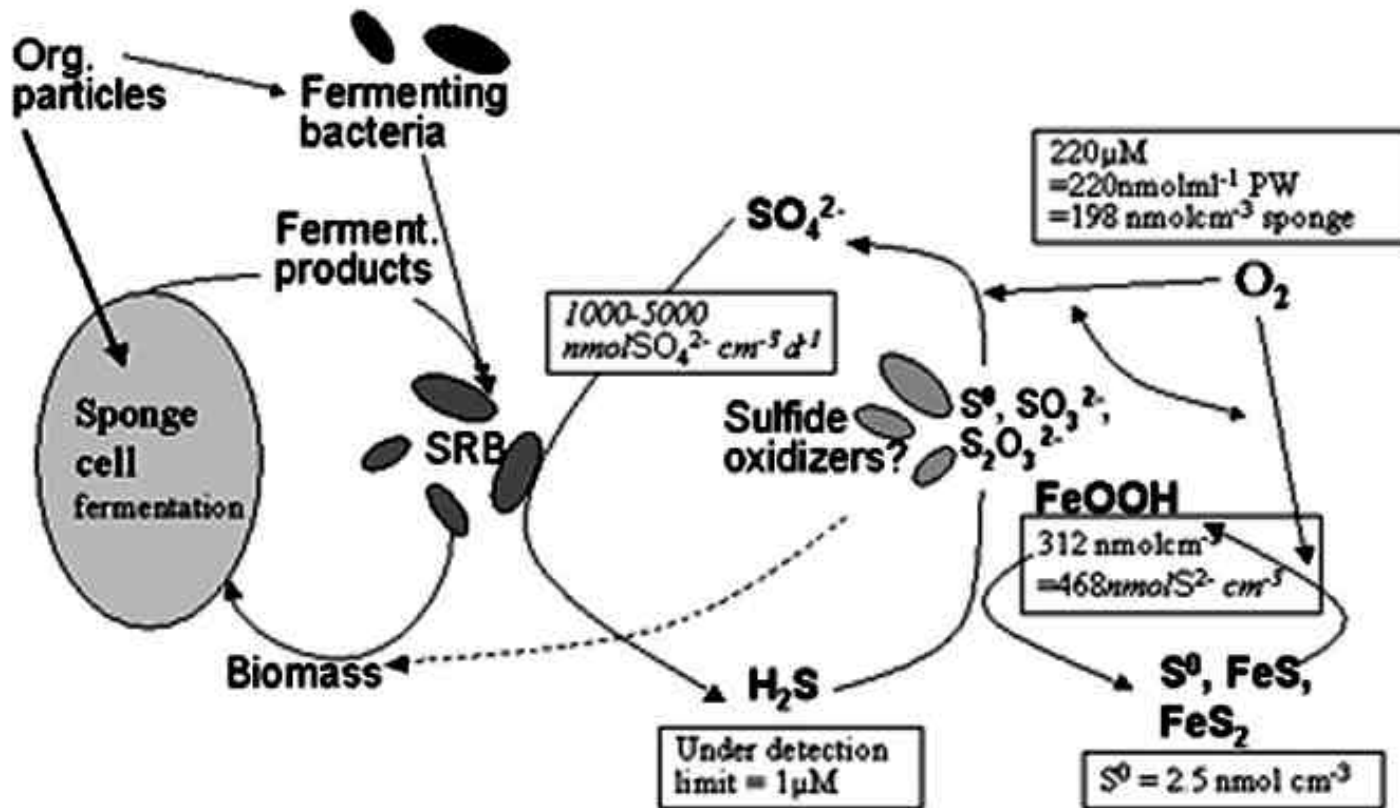
Microbial sulfate reduction in the tissue of the cold-water sponge Geodia barretti (Tetractinellida, Demospongiae), Hoffmann F., Dissertation, Göttingen, 2003

Table 2. Sponges and their symbiotic microorganisms producing natural products

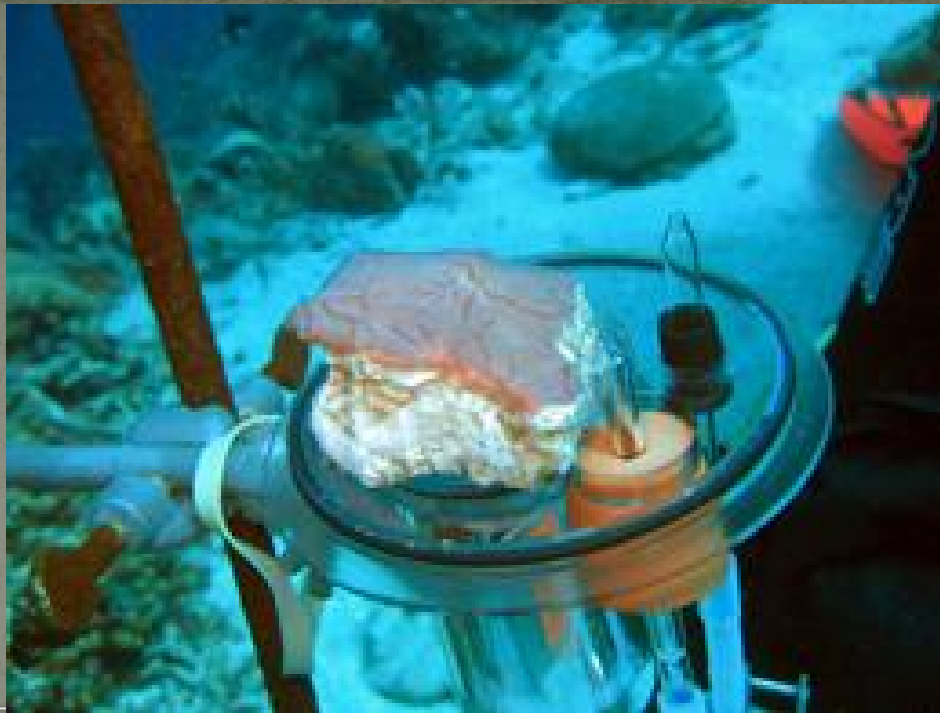
Sponge	Symbiotic microorganism*
<i>Aciculites orientalis</i>	Filamentous bacteria
Antarctic sponge	B, <i>Pseudomonas aeruginosa</i>
<i>Aplysina</i> sp.	B, <i>Arthrobacter</i> sp.
<i>Aplysina</i> sp.	B, <i>Bacillus</i> sp.
<i>Aplysina</i> sp.	B, <i>Micrococcus</i> sp.
<i>Aplysina</i> sp.	B, <i>Pseudoalteromonas</i> sp.
<i>Aplysina</i> sp.	B, <i>Vibrio</i> sp.
<i>Cenarchaeum symbiosum</i>	Archaeon
<i>Dysidea herbacea</i>	Cyanobacterium
<i>Dysidea herbacea</i>	C, <i>Oscillatoria spongeliae</i>
<i>Dysidea</i> sp.	B, <i>Vibrio</i> sp.
<i>Halichondria okadai</i>	B, <i>Alteromonas</i> sp.
<i>Halichondria okadai</i>	D, <i>Prorocentrum lima</i>
<i>Halichondria panicea</i>	B, <i>Antarcticum vesiculatum</i>
<i>Halichondria panicea</i>	B, <i>Pseudomonas insolita</i>
<i>Halichondria panicea</i>	B, <i>Rhodobacter</i> sp.
<i>Halichondria panicea</i>	B, <i>Psychroserpens burtonensis</i>
<i>Homophymia</i> sp.	B, <i>Pseudomonas</i> sp.
<i>Hyatella</i> sp.	B, <i>Vibrio</i> sp.
<i>Rhopaloeides odorabile</i>	B, β -Proteobacteria
<i>Rhopaloeides odorabile</i>	B, γ -Proteobacteria
<i>Rhopaloeides odorabile</i>	A, Actinobacteria sp.
<i>Rhopaloeides odorabile</i>	B, <i>Cytophaga</i> sp.
<i>Rhopaloeides odorabile</i>	Green sulfur bacteria
<i>Sigmadocia symbiotica</i>	R, <i>Ceratodictyon spongiosum</i>
<i>Suberea creba</i>	B, <i>Pseudomonas</i> sp.
<i>Suberea creba</i>	B, <i>Pseudomonas</i> sp.
<i>Tedania ignis</i>	B, <i>Micrococcus</i> sp.
<i>Theonella swinhoei</i>	B, δ -Proteobacteria
<i>Theonella swinhoei</i>	C, <i>Aphanocapsa feldmanni</i>
<i>Theonella swinhoei</i>	Filamentous bacteria
<i>Theonella swinhoei</i>	Unicellular bacteria
Unidentified sponge	A, <i>Streptomyces</i> sp.
<i>Verongia</i> sp.	B, <i>Aeromonas</i> sp.
<i>Verongia</i> sp.	B, <i>Pseudomonas</i> sp.
<i>Xestospongia</i> sp.	B, <i>Micrococcus luteus</i>



Schematic diagram of symbiotic relationships between sponges and microorganisms. A, extracellular exosymbiosis; B, extracellular endosymbiosis; C, intracellular symbiosis; and D, intranuclear symbiosis. Microbial Symbiosis in Marine Sponges, Lee *et al.* J. Microbiol., Vol. 39, No. 4, 254-264.



Biological-chemical and sponge-bacteria interactions in the tissue of *G. barretti*.
Microbial sulfate reduction in the tissue of the cold-water sponge Geodia barretti
 (Tetractinellida, Demospongiae), Hoffmann F., Dissertation, Göttingen, 2003



How the sponge stays slim, *Nature* / doi:10.1038/news.2009.1088
One species' rapid cell shedding explains its huge carbon-catching capacity.

De Goeij, J. M. *et al.*, *Cell kinetics of the marine sponge Halisarca caerulea reveal rapid cell turnover and shedding. J. Exp. Biol.* 212, 3892-3900 (2009)

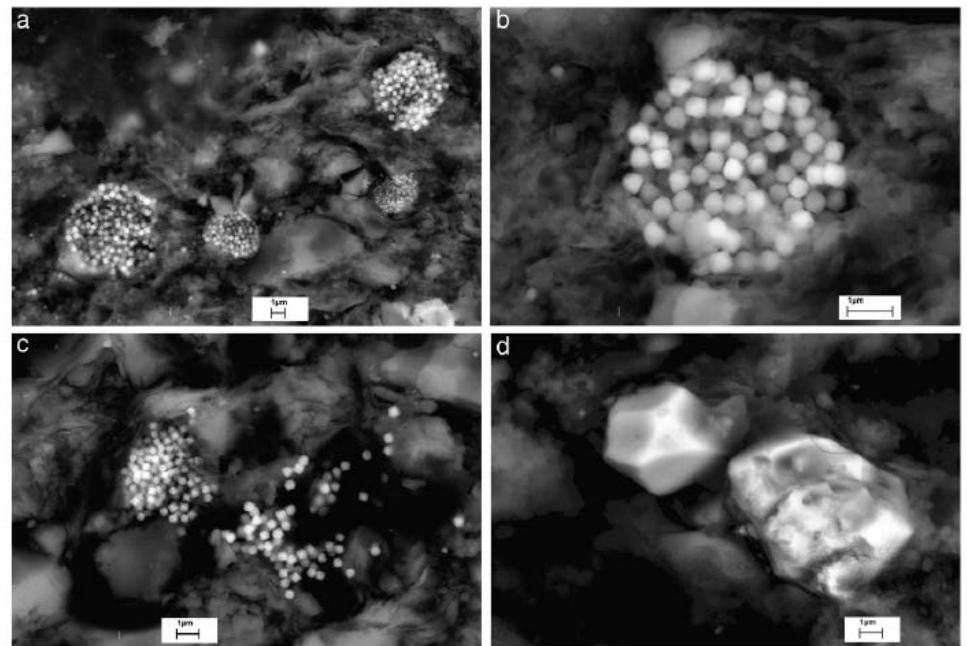
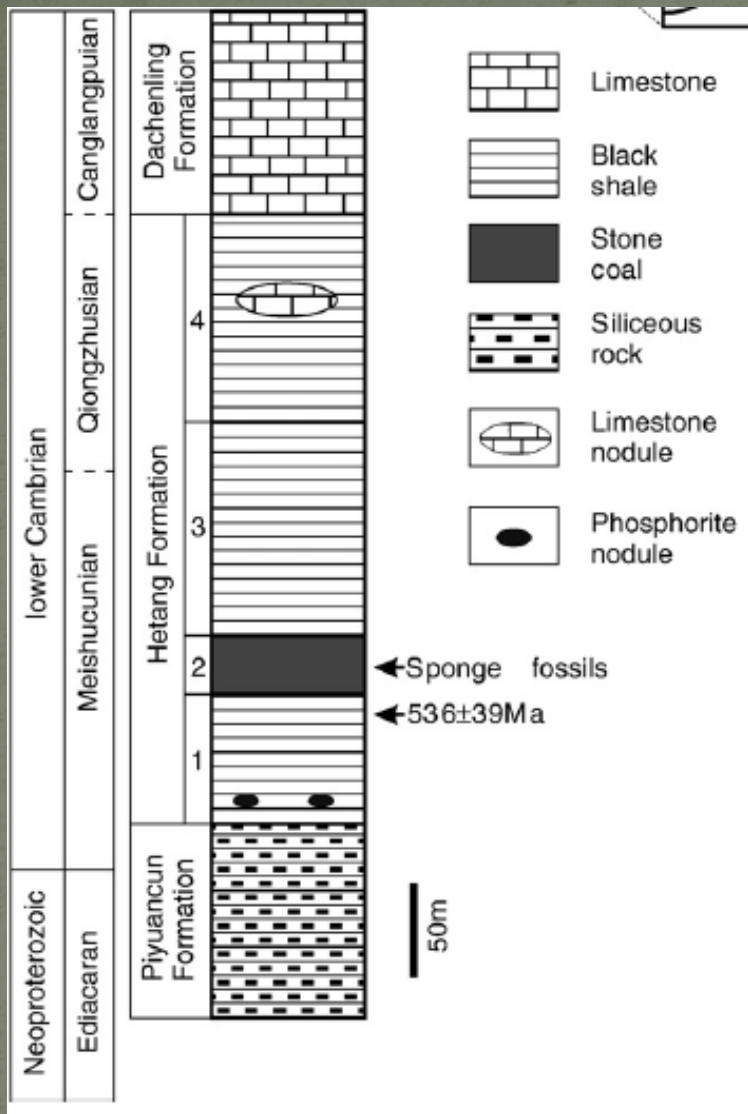


Fig. 2. Backscattered electron (BSE) images of closely packed, typical pyrite framboids (a, b), less dense packed framboids (c), and later diagenetic pyrite crystals (d).

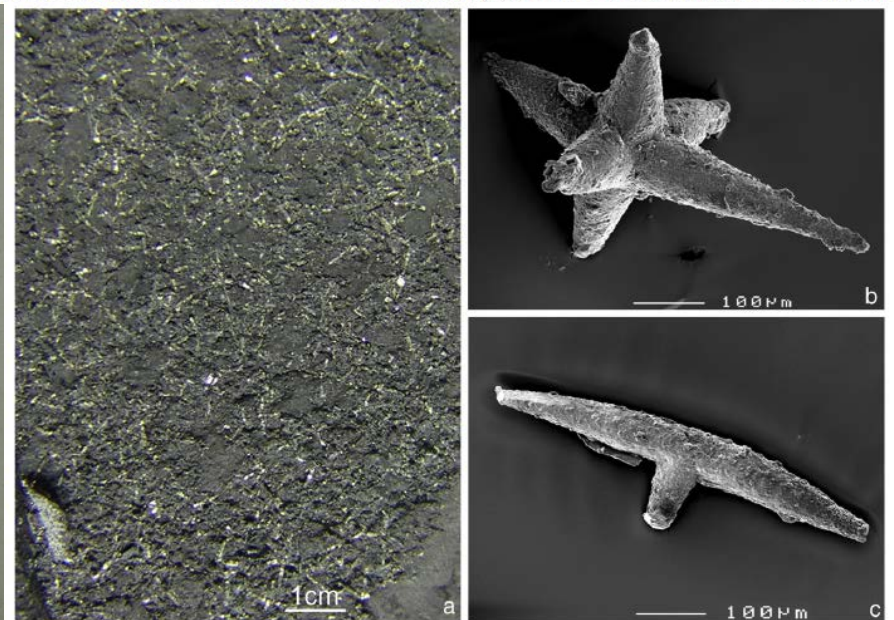
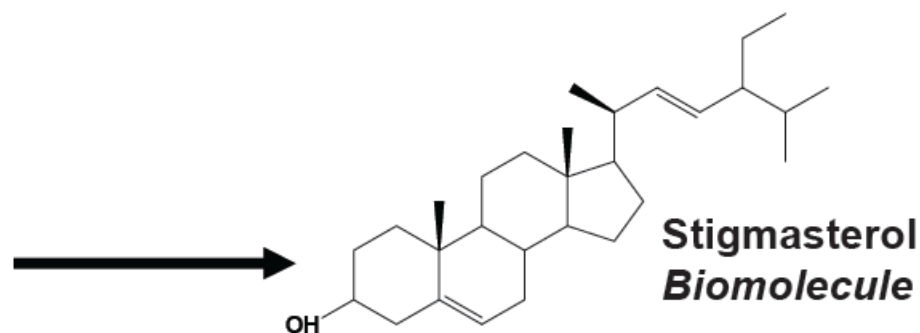
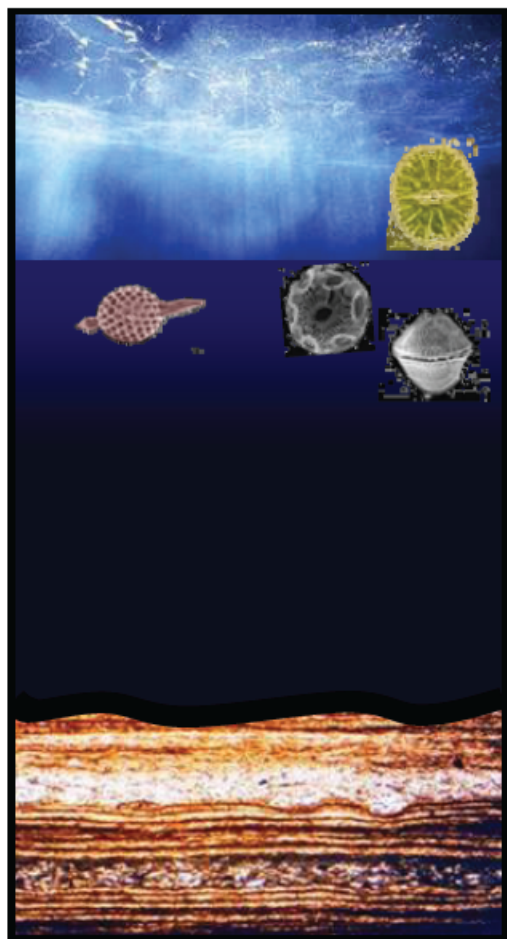


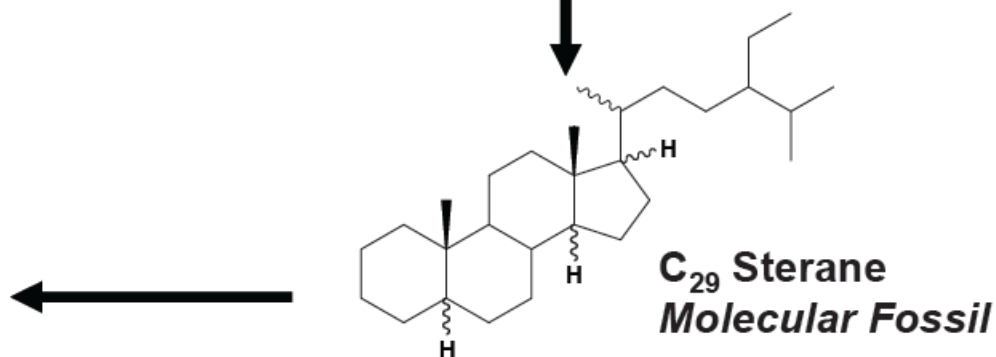
Fig. 7. Pyritized sponge spicules. a, pyritized spicules on the rock bedding planes; b, c, SEM photographs of pyritized spicules.

The Biomarker Principle



**Destruction of
Labile Compounds
(Nucleic Acids, Proteins)**

**Burial,
Diagenesis,
Temperature**



**Loss of functional groups, unsaturation;
Informative alteration of stereochemistry**

- **Petroleums and bitumens from Early Proterozoic (1800 Ma) to Miocene (15 Ma) age marine strata contain 24-isopropylcholestanes**, a novel group of CsO steroids. The abundance of these compounds, relative to 24-n-propylcholestanes, varies with source rock age. Late Proterozoic (Vendian) and Early Cambrian oils and/or bitumens from Siberia, the Urals, Oman, Australia, and India have a high ratio of 24-isopropylcholestanes to 24-n-propylcholestanes (>1), while younger and older samples have a lower ratio (<0.4). **Temporal changes in this parameter may reflect the relative abundance of certain Porifera (sponges) and certain marine algae through time**. Geochemical indicators such as this, which can constrain the source rock age of a migrated oil, are useful in source rock identification during petroleum exploration.

Paleoenvironmental implications of novel CM steranes in Precambrian to Cenozoic age petroleum and bitumen, McCaffrey et al., *Geochimica et Cosmochimica Acta*, 1994, Vol. 58, pp. 529-532

Table 1 Distributions of selected biological markers in reef carbonates and associated organisms

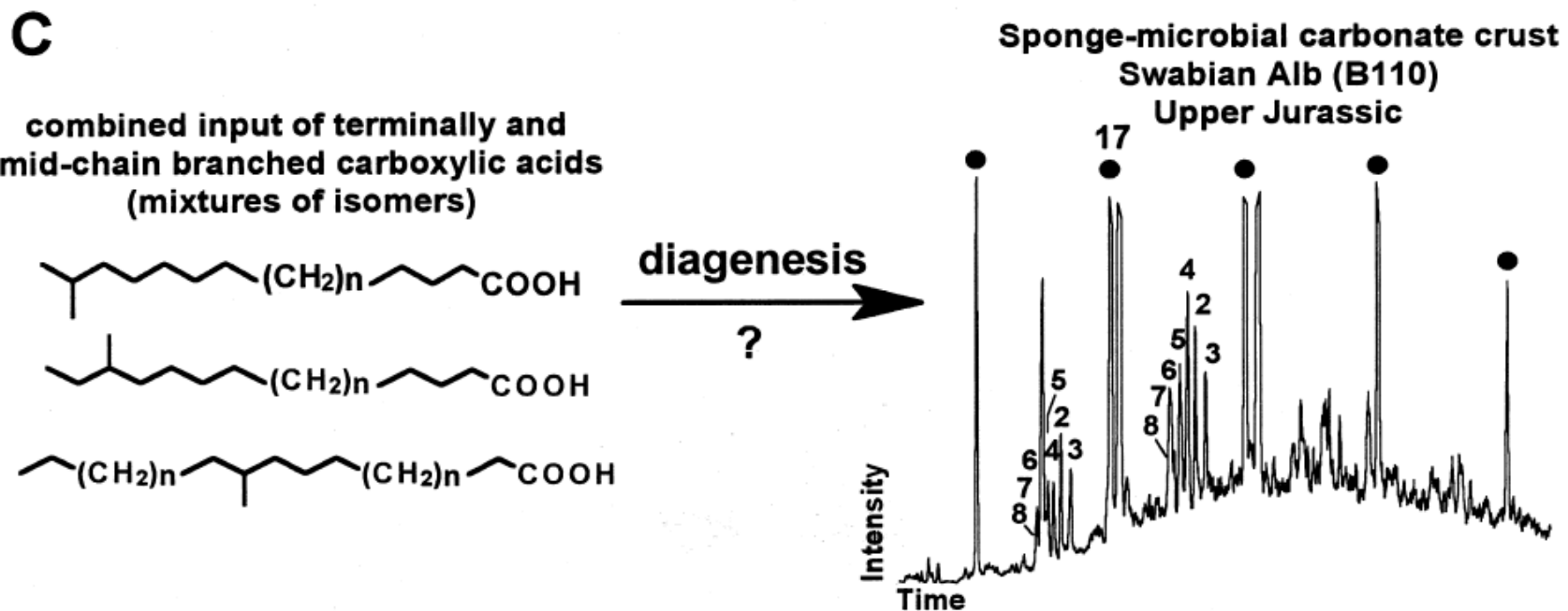
COMPOUND	STRUCTURE	FEATURE	ORIGIN	SAMPLES									
				'Cyanobacterial facies'			Reef carbonates (marine)		Sponges				
				Cultures	Carbonates (recent)	Carbonates (mature)	Microbialites	Others	Agelassids	Others			
<i>n</i> -Heptadecane		high relative abundance	Cyanobacteria		XX XX XX XX	X X X XX							
<i>n</i> -Heptadecenes		high relative abundance	Cyanobacteria	XX XX	XX XX XX XX		tr XX						
<i>n</i> -Octadecenes		high relative abundance	Green algae (?)		X X XX X		XX XX						
Mid-chain br. alkanes		discrete isomers	Cyanobacteria		XX XX XX XX	tr XX X X							
Dimethyl-alkanes		presence	Cyanobacteria		X		XX						
Diploptene		high relative abundance	Cyanobacteria	X	X X XX X	XX XX X X							
Short-chain <i>n</i> -alkanes		modal distributions	Metabolites?					XX XX XX XX X	XX XX			X	X
Mid-chain br. alkanes		complex mixtures	Metabolites?					tr XX XX XX X	X X			X	tr
Linear fatty acids <C25		high relative abundance	widespread	XX XX	XX XX XX XX	XX XX XX XX	XX XX XX XX X	XX XX	XX XX	XX XX XX XX X	XX XX		
Terminally br. fatty acids		presence	Anoxygen. bacteria		X X X tr	O X X X	tr XX XX X XX	X X	XX XX XX XX XX XX	tr			
Mid-chain br. fatty acids		presence	Heterotr. bacteria		tr X X	O tr X tr	XX XX tr XX	tr	XX XX XX XX XX XX	tr			
Demospionic acids		presence	Demospunges			X O	XX XX	XX		XX XX XX XX XX XX			
Highly br. Isoprenoids		presence	Diatoms			XX							
Cholesterol		presence	Animals, algae		XX O	tr		O	XX XX	tr	XX XX		XX XX
Δ7-Sterols		presence	Animals, sponges			O		O		tr		XX XX XX	X
Halogenated compounds		presence	Sponges			O		O	XX XX	tr		XX XX tr X tr	
<i>n</i> -alkanes >C25 (odd)		high relative abundance	Higher plants		X XX XX tr	XX XX XX X	X	tr tr XX X	tr tr			X	X

Explanations

XX = main compound / pronounced feature
 X = minor relative abundance / subordinate feature
 tr = trace compound
 o = compound fraction not analyzed
 no entry: compound / feature absent or below detection limit
 br. = branched

Thiel et al., (1996): Biogeochemistry of Modern Porifera and Microbialites from Lizard Island (Great Barrier Reef, Australia) and Fossil Analogues. In: Reitner et al., *Globale und regionale Steuerungsfaktoren biogener Sedimentation*, Gött.Arbeitskreis Paläontologie, SB2, 129-132; Göttingen.

“The found mid-chain branched carboxylic acids represent potential biological precursors for series of mid-chain branched alkanes present in ancient sediments and oils”



Mid-chain branched alkanolic acids from “living fossil” demosponges: a link to ancient sedimentary lipids? / Thiel et al. *Organic Geochemistry* 30 (1999) 1-14.

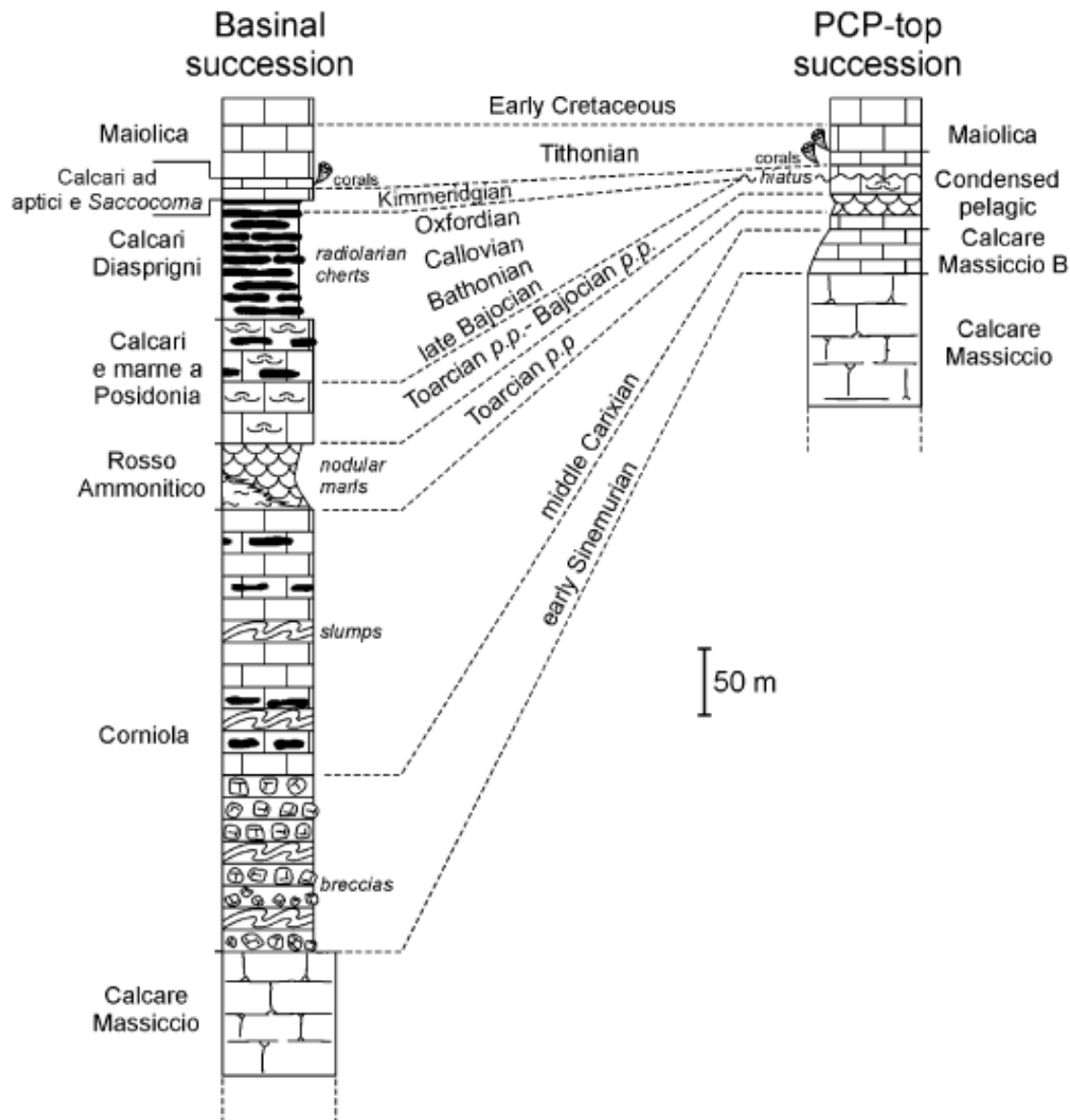
LETTERS

Fossil steroids record the appearance of Demospongiae during the Cryogenian period

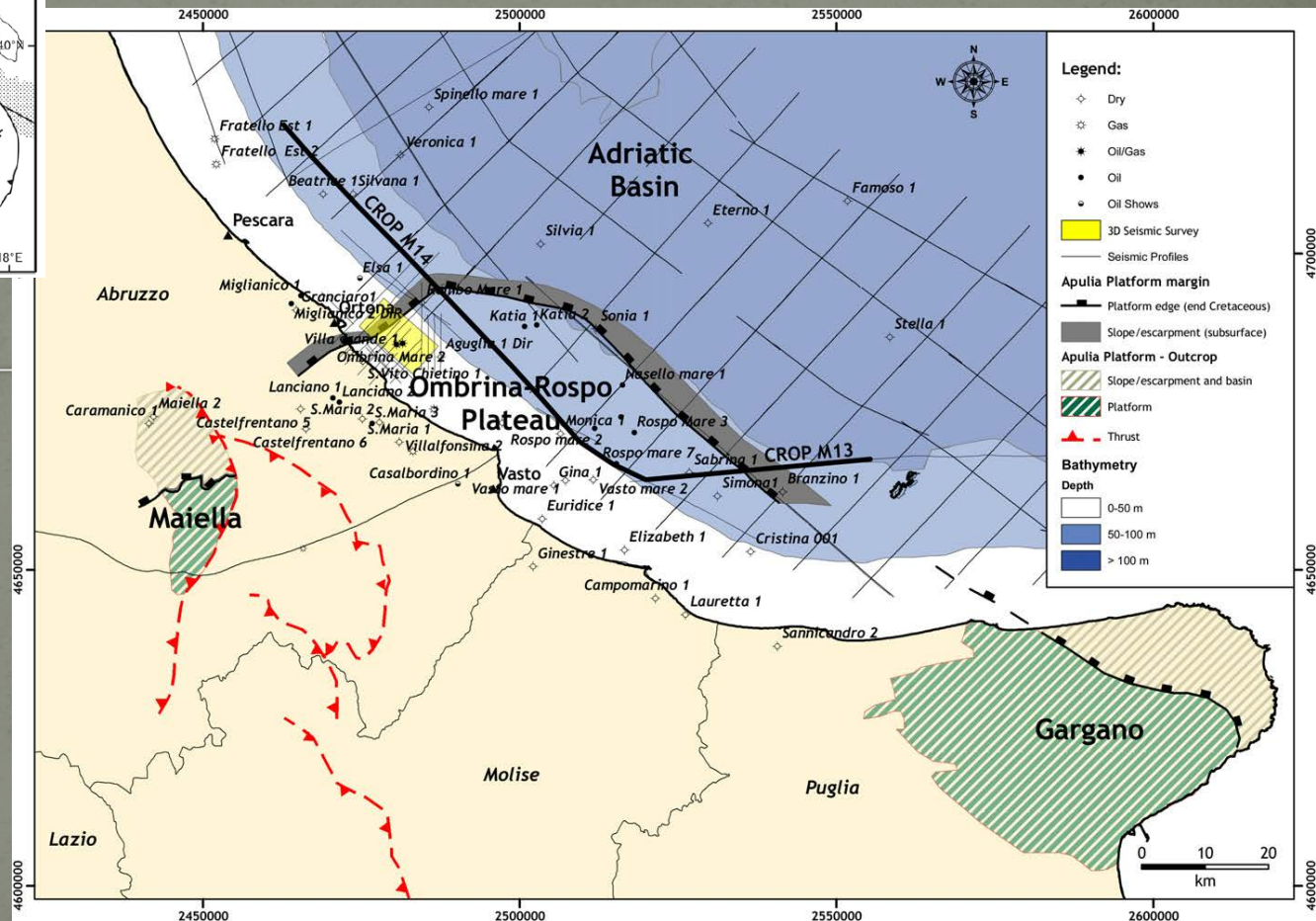
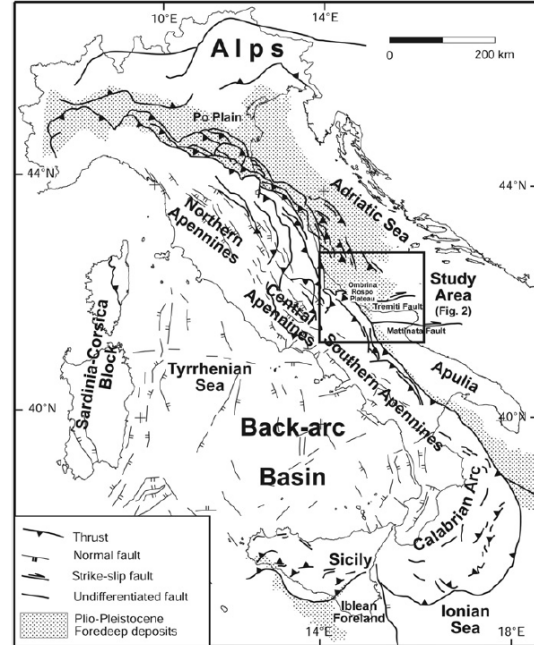
Gordon D. Love^{1,2}, Emmanuelle Grosjean³, Charlotte Stalvies⁴, David A. Fike⁵, John P. Grotzinger⁵, Alexander S. Bradley², Amy E. Kelly², Maya Bhatia², William Meredith⁶, Colin E. Snape⁶, Samuel A. Bowring², Daniel J. Condon^{2†} & Roger E. Summons²

“...C30 steranes comprised 2.7% of total C27–C30 extractable steranes in Huqf samples and 63% of the summed C30 compounds were 24-isopropylcholestanes, suggesting that demosponges must have made a significant contribution to preserved sedimentary organic matter...”

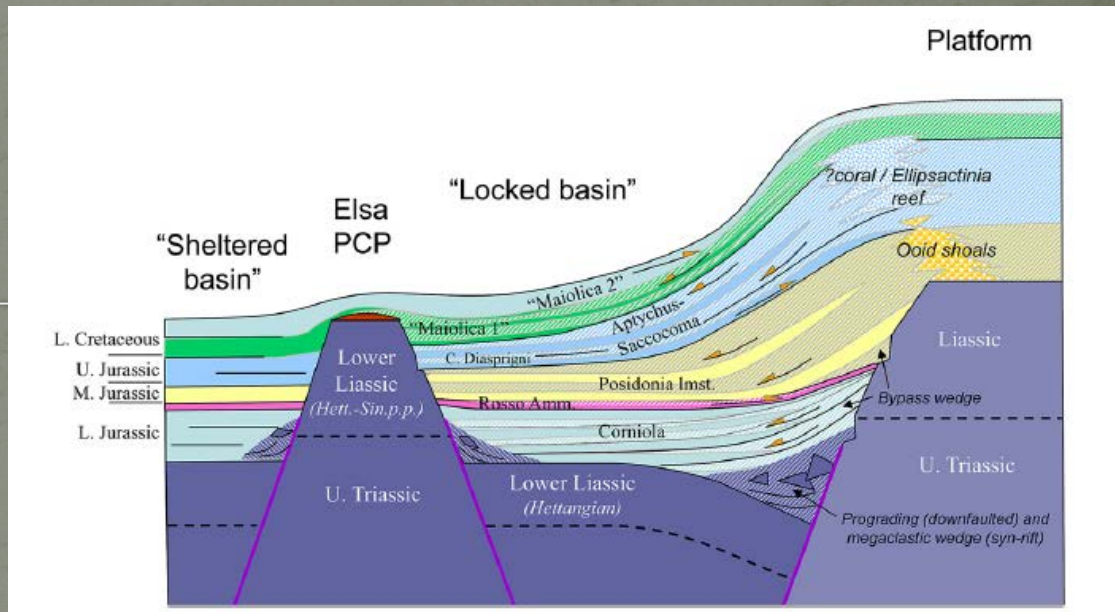
Name	Area	Stratigraphical position	References
Formal names			
Lombardian Maiolica Fm.	Lombardian Alps	U. Tithonian – Barremian	Weissert, 1979, 1981
Russenna – Aptychenkalk Fm.	Central Alps (Austroalpine units)	U. Tithonian – L. Aptian	Dössegger <i>et al.</i> , 1982
Pieniny Limestone Fm.	Pieniny Klippen Belt	Tithonian – Barremian	Birkenmajer, 1977
(?) Lucivna Fm.	Western Inner Carpathians	U. Berriasian – L. Albian	Polák & Bujnovsky, 1979
Murguceva Fm.	S. Carpathians	Tithonian – Hauterivian	Avram, 1976, 1984
Mogyrosdomb Limestone Fm.	Bakony	Tithonian – L. Barremian	Kazmer, 1986
Márevar Limestone Fm.	Mecsek	U. Tithonian	Kazmer, 1986
Chiaramonte Fm.	SE Sicily	U. Tithonian – L. Hauterivian	Patacca <i>et al.</i> , 1979
Moro Fm.	Maio, Cape Verde Islands	Tithonian – Albian	Robertson, 1984a
Blake-Bahama Fm.	Blake-Bahama Basin	U. Tithonian – Barremian	Iansa <i>et al.</i> , 1979
(?) Tumbitas Mb. (Guasasa Fm.)	Sierra de Los Organos, Cuba	U. Berriasian – L. Hauterivian	Pszczółkowski, 1978
(?) Sumidero Mb. (Artemisa Fm.)	Sierra del Rosario, Cuba	Berriasian – Hauterivian	Pszczółkowski, 1978
Informal names			
Venetian Biancone Fm.	Venetian Alps	U. Tithonian – L. Aptian	Weissert, 1981
Maiolica Fm.	Southern Alps	U. Tithonian – L. Aptian	Baumgartner, 1984; Renz Habicht, 1985
Calcare di Soccher (partly)	A. Alps (Belluno)	Oxfordian – Campanian	Gnaccolini, 1968; Casati & Tomai, 1969
Calcare Rupestre	Apennines	U. Tithonian – L. Aptian	Bartolotti <i>et al.</i> , 1970
Lattimusa	Sicily	U. Tithonian – L. Cretaceous	Wendt, 1969
Vigla Limestone (partly)	Hellenides	Tithonian – M. Cretaceous	Bernoulli, 1972
Aptychenkalk	Northern Calcareous Alps (Albania)	Tithonian – Berriasian	Prey, 1980
Oberalm Beds	Northern Calcareous Alps	U. Tithonian – M. Cretaceous	Patzelt, 1971
Svaljavaska svita	Pieniny Klippen Belt (Ukrainian sector)	Tithonian – L. Berriasian	Flügel & Fenninger, 1966; Garrison, 1970
		Tithonian – L. Barremian	Kruglov, 1979
Hornsteinkalk (old name)	Pieniny Klippen Belt	Tithonian – Barremian	see Birkenmajer, 1977



Lithostratigraphic and geochrono-correlation across an end-member PCP succession and a basinal succession in the Umbria– Marche and Sabina Apennines, Gill et al., *Sedimentary Geology* 166 (2004) 311–334



FORMATIONS (BASIN)	STAGES	BIOZONES (INNER PLATFORM)	BIOZONES (PLATFORM MARGIN)
Scaglia Rossa	Maastrichtian	Discorbiidae and Miliolidae	Orbitoides
	Campanian	Orbitoides media	
	Santonian	Discorbiidae and Ostracoda	Radiolitiidae and Hippuritidae
	Coniacian	Accordiella conica and Rotorbinella scarsellai	
	Turonian	Nezazatinella cf. aegyptiaca and Numuloculina cf. irregularis Ch. gradata and P. reicheli	
Scaglia Bianca	Cenomanian	P. dubia and P. lauricensis	Orbitolina
Mare a Fuocidi	Albian	Ostracoda and Miliolidae Dictyoconus algerianus	
	Aptian	Archaealveolina reicheli Salpingoporella dinarica	
Maiolica	Barremian	?Cuneolina scarsellai and Cuneolina composaurii	Lithocodium aggregatum
	Hauterivian	Cuneolina composaurii	
	Valanginian	Favreina salevernis and Salpingoporella annulata	
	Berriasian	Salpingoporella annulata	
Calcarei ad aptici e Saccocoma	Tithonian	Clypeina jurassica	Tubiphytes morronensis
	Kimmeridgian		
Calcarei Diasprigni	Oxfordian	Kurmubia gr. palastiniensis	Protopenereplis striata
	Callovian		
Calcarei e marna a Posidonia	Bathonian	Palaeopleroderina salernitana Redmondioidea	Gutnicella cayuxi
	Bajocian	Selliporella donzellii	
	Aalenian	Bosnicella croatica Echinodermata, Mollusca and Favreina	
	Toarcian		
Rosso Ammonitico	Pliensbachian	Palaeodasycladus mediterraneus	Palaeodasycladus mediterraneus and Rivularia piae
Comiola	Sinemurian		
	Calcare Massiccio	Hettangian	Thaumatoporella parvovesiculifera



The north-western margin of the Ombrina Plateau and Elsa high restored; Jurassic and Lower Cretaceous. Not to scale

Σας ευχαριστώ πολύ για
την προσοχή σας